IBIS

Final Proposal
Undergraduate Design Team
University of Maryland, College Park

41st Annual Vertical Flight Society Student Design Competition

Sponsored by DEVCOM ARL

Alfred Gessow Rotorcraft Center

Department of Aerospace Engineering

University of Maryland

College Park, MD 20742

Emma Farren

Undergraduate Student (Team Lead)

efarren@umd.edu

Javier Turuelo Menéndez

Undergraduate Student (CAD)

jturuelo@umd.edu

Aidan Hayes

Undergraduate Student (Avionics)

ahayes17@umd.edu

Visesh Uppoor

Undergraduate Student (Aerodynamics)

vuppoor@umd.edu

Faith Pak

Undergraduate Student (Structures)

fpak@umd.edu

Howard Zheng

Undergraduate Student (Aerodynamics)

hzheng17@umd.edu

Jacques Read

Undergraduate Student (Powertrain)

jread7@umd.edu

Dr. Vengalattore Nagaraj

Faculty Advisor

vnagaraj@umd.edu

Students will receive credits for ENAE482 (Aeronautical Systems Design) for their contributions.

Alfred Gessow Rotorcraft Center

Department of Aerospace Engineering

University of Maryland

College Park, MD 20742

To the Vertical Flight Society:

The members of the University of Maryland Undergraduate Student Design Team hereby grant full permission to distribute the Executive Summary and Final Proposal for the 41st Annual Design Competition as they see fit.

Sincerely,

The UMD Undergraduate Design Team

Acknowledgements

The University of Maryland's undergraduate team wishes to acknowledge the support of the following people for their invaluable insight, guidance, time, and support throughout the design process.

University of Maryland Faculty and Staff

- *Dr. Vengalattore Nagaraj* - Research Scientist, Department of Aerospace Engineering
- *Dr. Inderjit Chopra* - Alfred Gessow Professor and Distinguished University Professor, Director of Alfred Gessow Rotorcraft Center, Department of Aerospace Engineering
- *Dr. James Baeder* - Igor Sikorsky Distinguished Professor in Rotorcraft Professor, Department of Aerospace Engineering
- *CDR Spencer Fishman, USN* - Aerospace Engineering Graduate Student, AGRC

Contents

List of Tables

List of Figures

Nomenclature

English Symbols

AR	Aspect Ratio
CG	Center of Gravity
C_T	Coefficient of Thrust
E	Young's Modulus
FM	Figure of Merit
L/D	Lift-to-Drag Ratio
M_{tip}	Tip Mach Number

Greek Symbols

η	Powerplant Efficiency
ρ	Density
σ	Solidity
σ_t	Ultimate Tensile Strength
σ_y	Yield Strength

Abbreviations

AHP	Analytical Hierarchy Process
BEMT	Blade Element Momentum Theory
BLOS	Beyond Line of Sight
CFD	Computational Fluid Dynamics
ConOps	Concept of Operations
FLIR	Forward Looking Infrared
FOV	Field of View
GNSS	Global Navigation Satellite System
GPS	Global Positioning System
GTOW	Gross Take-Off Weight
INS	Inertial Navigation System
LCV	Lower Calorific Value
LWIR	Long Wave Infrared
NDARC	NASA Design and Analysis of Rotorcraft
OASPL	Overall Sound Pressure Level
PELZ	Predetermined Emergency Landing Zone
RFP	Request For Proposal
ROC	Rate of Climb
RPM	Revolutions per Minute
SATCOM	Satellite Communication
SFC	Specific Fuel Consumption
SLAM	Simultaneous Localization and Mapping
SMR	Single Main Rotor
TRL	Technological Readiness Level
UAS	Unmanned Aerial System
UAV	Unmanned Aerial Vehicle
VBE	Velocity for Best Endurance
VBR	Velocity for Best Range
VM	Virtual Machine
VTOL	Vertical Take-off Landing

1 Introduction

The world is experiencing an increase in the frequency and intensity of natural disasters [1]. These hurricanes, tornadoes, wildfires, and earthquakes all isolate affected people from life-saving aid by destroying roads, runways, and communication infrastructure. Traditional ground vehicles and aircraft, each of which respectively require roads and runways, are unable to reach key locations due to these limitations. In the past decade, unmanned aerial vehicles (UAVs) have become more common as disaster response tools and rescue devices, acting as emergency responders to provide help in the aftermath of these natural disasters. Uncrewed vertical takeoff and landing (VTOL) aircraft have the ability to be quickly deployed, reach remote and dangerous locations, provide real time data, and connect victims to the next step towards rescue [2].

The Vertical Flight Society's 41st Annual Student Design Competition, sponsored by the U.S. Army Combat Capabilities Development Command Army Research Laboratory (DEVCOM ARL), tasks teams to design a multi-mission, modular, VTOL unmanned aerial system (UAS) as a means to quickly respond after natural disasters and access hard to reach places in an effort to provide immediate relief and support. The request for proposals (RFP) specified that this UAV must have the ability to takeoff and land vertically on the deck of a ship in both high winds and gusty conditions, cruise to the disaster site within 75 minutes, and to serve as a long-endurance communications relay or deliver relief supplies at the desired area of operation. These specifications outline the mission profiles and vehicle capabilities.

In response to this year's RFP, the University of Maryland and Universidad de Carlos III have developed *Ibis*, a lightweight, single main rotor UAV designed to be the first on the scene after a natural disaster. The aircraft is named after the White Ibis, a wading bird native to the Gulf Coast of North America (Figure 1). The White Ibis is known in Native American folklore to be the last animal to seek shelter before a hurricane and the first creature to return after the storm. The *Ibis* aircraft will be known for the same, operating as a reliable beacon of hope as the true first responder to start providing aid via supplies delivery or communications support after a natural disaster.

Fig 1: North American White Ibis

1.1 RFP Analysis

The RFP details two distinct mission profiles. The first, a supplies delivery beginning and ending on the deck of a ship over 185 km away from the delivery target, as shown in Figure 2. The second, Figure 3, is a long endurance mission where *Ibis* is tasked with loitering for a minimum of 10 hours in order to act as a communications relay.

Additional constraints the design team noted were sizing limitations for the takeoff and landing footprint (6x6 m), vehicle storage (4 aircraft in a 4x12x6 m hangar space), long endurance mission payload dimensions (0.05 m^3 cube), and a Gross Takeoff Weight (GTOW) of 160 kg exactly.

Ibis: First Bird Out, Last One Back

Proven and Available Technologies

- High Technological Readiness for All Components

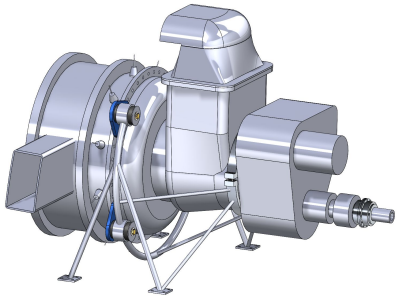

Highly Efficient Aerodynamic Design Enables Exceptional Performance

- High Performing Rotor
- Streamlined Fuselage
- Low Drag Hub Fairing

Single Aircraft Configuration

- Rapid Multi-Mission Reconfiguration

Safe Autonomous Flight

- Controllable from Anywhere in the World
- Fly Safely in Unmapped Territories

Accessible for Untrained Operators

- Simple to load with minimal experience

Max Payload	59 kg (130 lbs)
Max Endurance	10.8 hours
Empty Weight Fraction	55%
Installed Power	36.8 kW (50 HP)
Cruise L/D	5.23

UNIVERSITY OF MARYLAND

External Dimensions

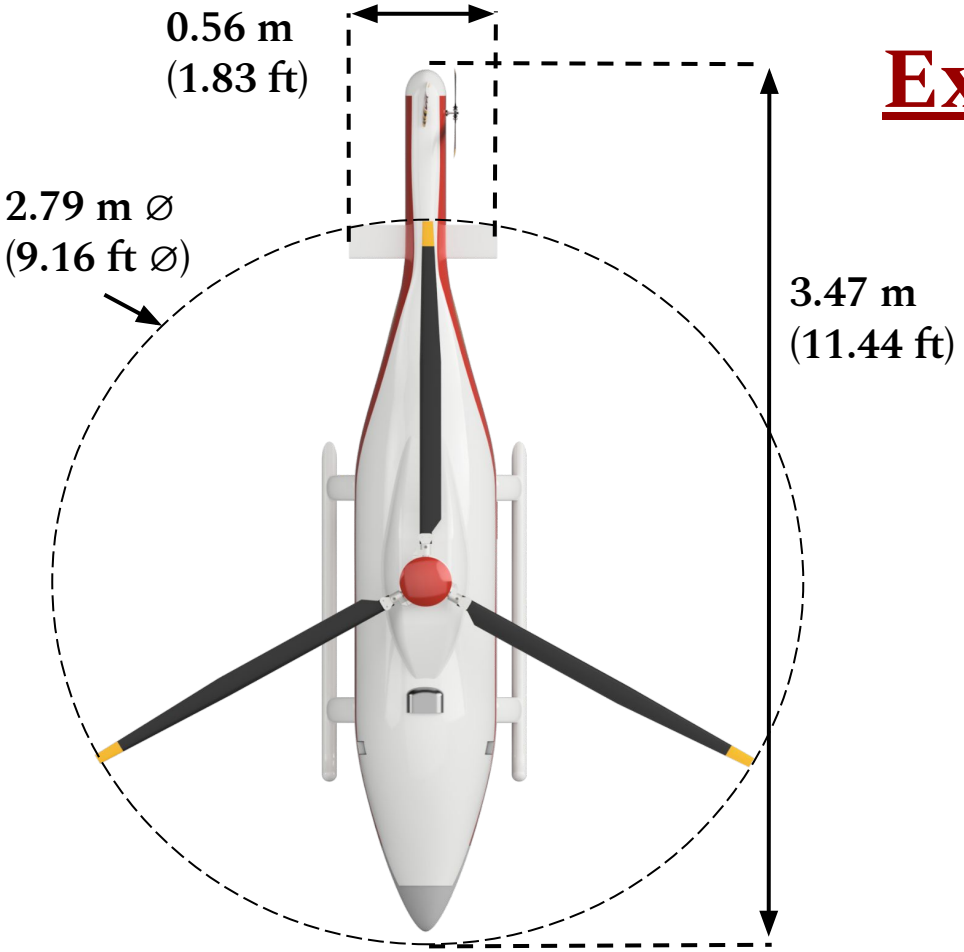

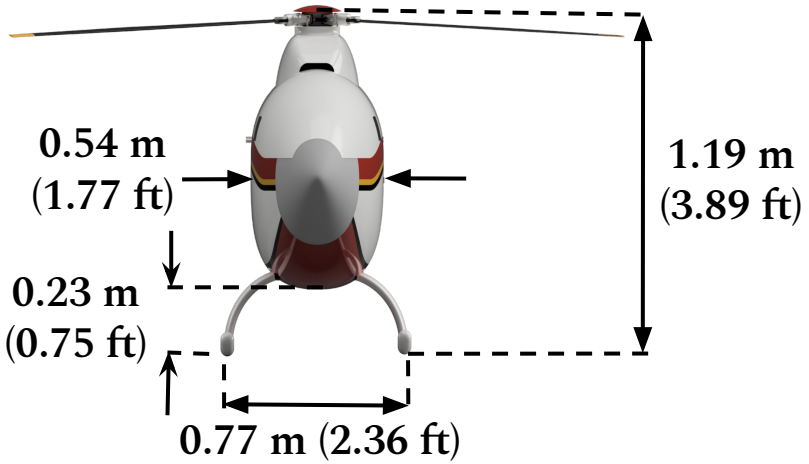

Footprint: 2.79 m x 3.47 m
(9.16 ft x 11.44 ft)

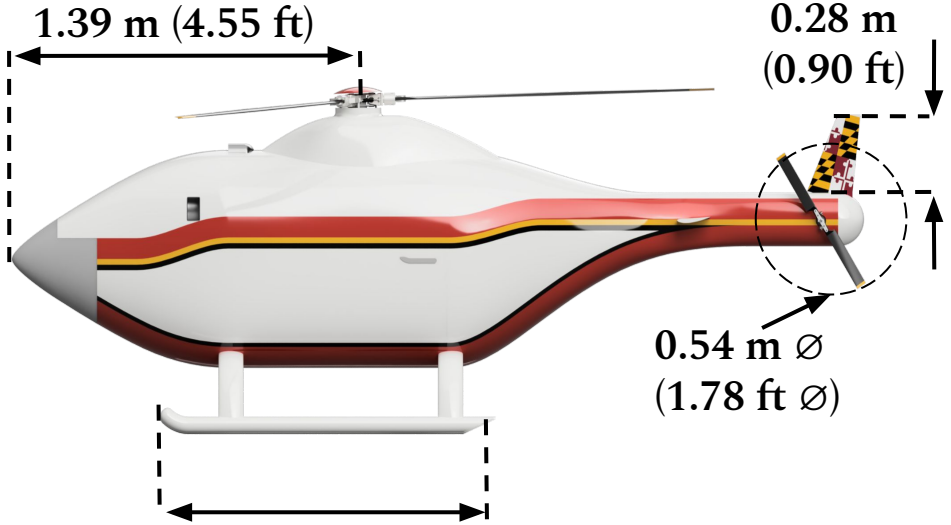

UNIVERSITY OF MARYLAND

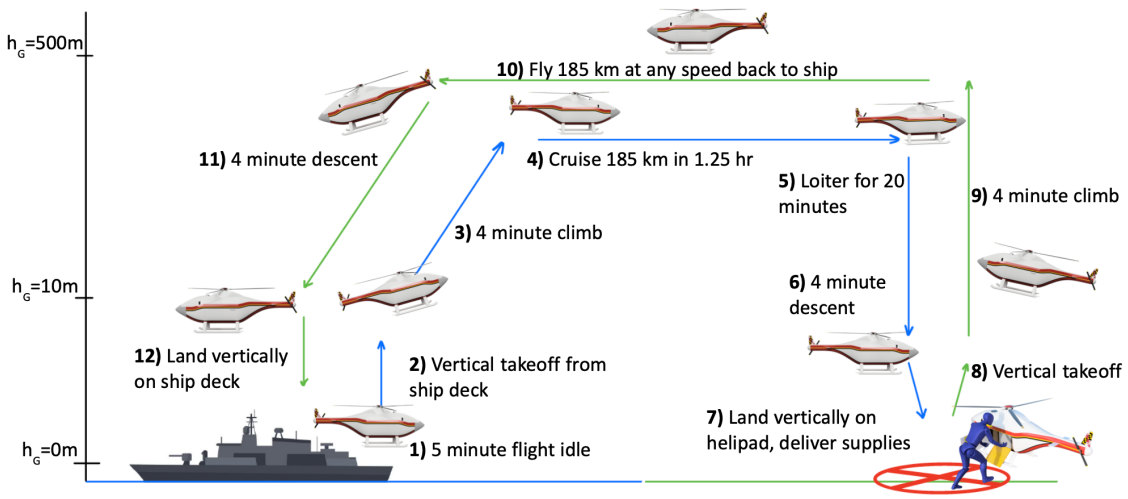

Fig 2: Supplies Delivery Mission

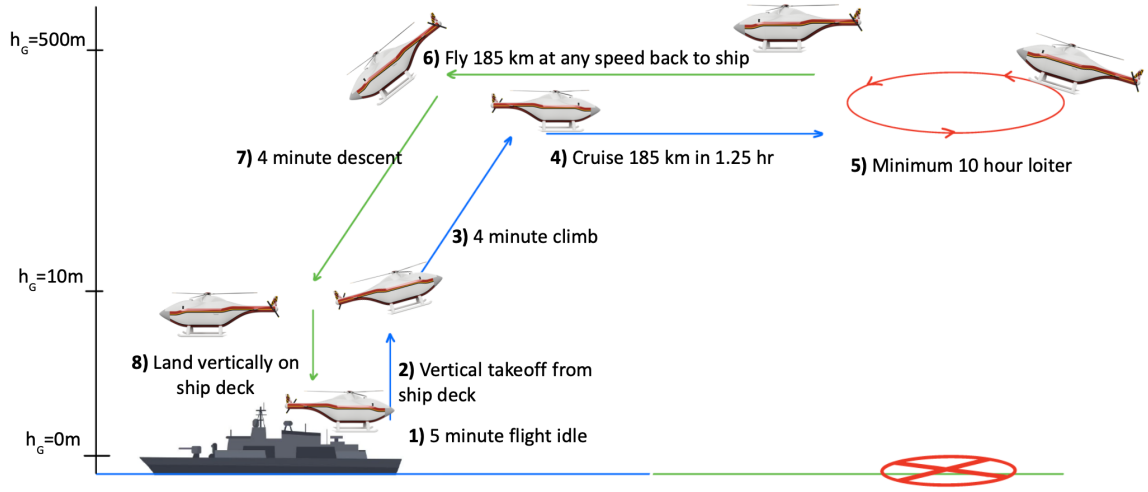

Fig 3: Long Endurance Mission

Along with the described missions, the following requirements were also specified:

- Required to be Jet-A fuel compatible
- Be maneuverable by 2 people using minimal equipment while on deck
- Tolerate head, cross, and tail winds and gusts

1.2 RFP Compliance

After a thorough review of the RFP, the requirements were placed into a chart. This ensured that the design process was directly guided by what the RFP requests. Table 1 shows which section in the report details each solution.

In addition to its primary purpose of serving in a disaster relief scenario, *Ibis* was designed to be used in applications such as commercial delivery, agriculture, search and rescue, geographical survey, and surveillance, so that it will not idle until a disaster strikes. This increases the economic viability of the design, making it a strong player in the UAV market (Figures 4 and 5).

Table 1: RFP Compliance

RFP Requirement	Section
Vehicle must takeoff and land in a 6x6 m footprint	3
Vehicle must takeoff and land on the deck if a ship in high-winds and gusty conditions	4.3
Cruise to and from disaster site 185 km away in 1.25 hours	10.2
Use minimal launch and recovery equipment	7.6
Vehicle must be able to complete more than one mission with base structure	2.4, 8
Have a spatial accuracy of 1m for recovery	9
Engine must be Jet-A compatible	6.1, 6.5
Support Payload & Accessories Bus Power up to 800 Watts	6.2

Fig 4: Agricultural Survey

Fig 5: Search and Rescue

2 Configuration Selection

With two distinct mission profiles, selecting a versatile and effective base configuration posed the first major challenge. To ensure the selection of the best configuration, a thorough analysis of the mission profiles and voice of the customer was conducted.

2.1 Voice of the Customer

An in-depth assessment of the RFP was carried out in order to fully understand the wants and needs of the customer. The team worked diligently to satisfy the different requirements of each mission. The supplies delivery mission requires the vehicle to carry a large payload that is over 30% of aircraft's gross takeoff weight (GTOW). At the same time, the endurance mission requires the vehicle to be efficient in fuel consumption and forward flight. The required gust tolerance, maritime operating environment, and small ground crew allotment creates a need for quick maneuverability, anti-corrosion measures, and safety to be desirable features.

2.2 Design Drivers

Using this reasoning, seven major design drivers were identified. These criteria informed and guided the team throughout the configuration selection and design process.

i. Efficiency in Forward Flight

The design must minimize weight and fuel consumption during the cruise to and from the target area as well as during the long endurance loiter.

ii. Controllability

Flying in wind gusts and operating on a ship deck both require a vehicle that is strictly controlled and responsive in order to maintain safe and stable flight.

iii. Marinization

Operating on the deck of a ship exposes aircraft to many corrosive elements that one operating solely over land would not encounter. The vehicle must be resistant to salt water corrosion, ozone, fluctuating temperatures, and miscellaneous particulate debris.

iv. Life Cycle Cost

Accounting for the life cycle cost of the rotorcraft, from development to disposal, was a major consideration when selecting materials and the complexity of the UAS.

v. Mechanical Simplicity

The vehicle must achieve the mission goals while keeping the design, control system, and overall function as simple as possible to maximize efficiency and reduce maintenance.

vi. Versatility

The RFP emphasized modularity, therefore the vehicle must be as versatile as possible and able to conduct a wide variety of missions with future modules in order to respond to future problems.

vii. Ground Crew Safety

Both a trained and presumably untrained ground crew will be operating in close proximity to the vehicle. The vehicle must therefore be safe and simple to work with and near. The vehicle must be maneuverable, and the modules could be swapped out with skills that the average sailor already has or could learn quickly and easily.

2.3 Analytical Hierarchy Process

In order to balance each design driver in the design process, an Analytical Hierarchy Process (AHP) was utilized. The AHP involves each team member comparing the relative importance of the design drivers and assigning weights on a scale of 1 to 10 (least important to most important). Table 2 shows one of the team member's assigned weights and Figure 6 shows the final weight results in a pie chart.

Table 2: Design Driver AHP

	Versatility	Efficiency in Flight	Controllability	Life-Cycle Cost	Marinization	Ground Crew Safety	Mechanical Simplicity
Versatility	1	3	1	5	3	2	0.6
Efficiency in Flight	0.33	1	0.6	8	0.5	1	0.1
Controllability	1	1.67	1	5	2	1	1
Life-Cycle Cost	0.2	0.13	0.2	1	0.3	0.2	0.1
Marinization	0.33	2	0.5	3.33	1	2	0.5
Ground Crew Safety	0.5	1	1	5	0.5	1	1
Mechanical Simplicity	1.67	10	1	10	2	1	1

As reflected in Figure 6, the *Ibis* team values the mechanical simplicity, versatility, and efficiency very highly throughout the design process. Although cost was ranked lowest in the AHP, this does not reflect that it was unimportant to the team, but that cutting costs was not a primary driver in our design choices for the *Ibis*. Efficiency in forward flight, mechanical simplicity, and controllability all imply low weight and low drag. In the actual design process low weight and aerodynamic efficiency were both a major drivers as well.

2.4 Configurations Considered

Seven aircraft configurations were considered as options in the next step of the team's evaluation process. Because reliability and mechanical simplicity were important factors, the team decided to look at four of the most conventional aircraft, to easily compare the existing data on power and performance of the biggest players on the market. The team also considered tail sitters, quadrotors, and compound helicopters which are less prevalent, but provide non-conventional insight into other options on how to deal with the RFP sizing limitations.

i. Single Main Rotor (SMR)

The SMR configuration is the most widely used and recognized rotorcraft configuration. Known for its reliability and safety, it is the simplest configuration that was considered.

ii. Coaxial

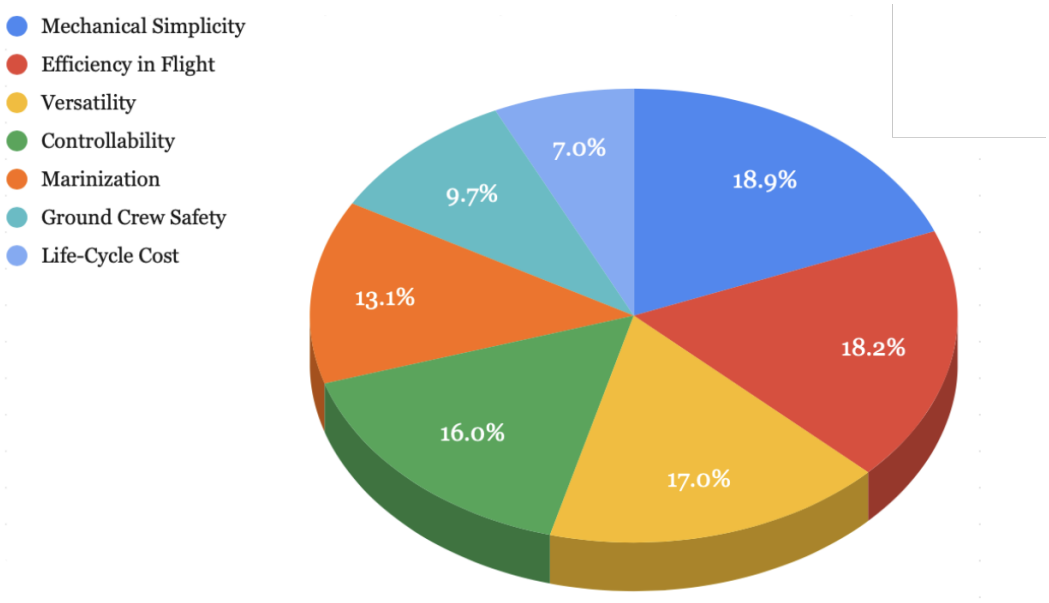

Fig 6: Design Driver Weights

The coaxial rotor configuration utilizes two stacked, counter-rotating rotors, removing the need for a tail rotor. However, the larger rotor hub greatly increases drag and mechanical complexity.

iii. Tandem

The tandem rotor configuration negates the need for a tail rotor while also allowing for a higher variance in the longitudinal center of gravity (CG). This comes at the cost of splitting the power between 2 rotors, adding complexity and extra points of failure.

iv. Tiltrotor

The tiltrotor configuration combines the efficient forward flight capabilities of a conventional fixed-wing airplane with the VTOL capabilities of rotorcraft. However, the mechanical complexity of tilting nacelles can be unreliable.

v. Tail Sitter

Tail sitter aircraft takeoff and land vertically using a rotor attached to the nose cone of the aircraft. When in forward flight, they rotate 90° to operate as a winged aircraft. They also require an enormous amount of control to be able to safely and reliably tilt into forward flight. In addition, this configuration is very new to the industry and is not very reliable at a large scale.

vi. Quadrotor

A quadrotor is a common design for commercial drones due to its flight stability and maneuverability. However, without a fuselage, whatever payload the aircraft is carrying creates a huge amount of drag at high speeds.

vii. Compound

A compound helicopter takes the familiarity of an SMR helicopter and combines it with the endurance of an airplane. The addition of wings for lift augmentation and a trailing propellor for thrust augmentation allows the aircraft to have a larger range and better fuel consumption. However, the design requires more maintenance and is more mechanically complex than other configurations.

These configurations were considered using a Pugh matrix. This compares various concepts with respect to how they perform against a set of criteria. The criteria against which these configurations were measured are the design drivers that were outlined in Section 2.2. The results are shown in Table 3. The SMR configuration was set as the control configuration, meaning every other configuration was ranked on a scale of -3 to 3 (absolutely worse to

Fig 7: Single Main Rotor

Fig 8: Coaxial Rotor

Fig 9: Tandem Rotor

Fig 10: Tiltrotor

Fig 11: Tail Sitter

Fig 12: Quadrotor

Fig 13: Compound

absolutely better) in comparison to SMR. The highest scoring configurations are then evaluated in a more in-depth analysis.

Table 3: Pugh Matrix

	Weight	SMR	Coaxial	Tiltrotor	Tandem	Tail Sitter	Compound	Quadrotor
Efficiency in Flight	0.18	0	1	2	1	-1	1	-1
Controllability	0.16	0	2	-1	1	-1	-2	3
Marinization	0.13	0	-2	-1	0	0	-1	-2
Versatility	0.17	0	0	1	0	1	2	0
Ground Crew Safety	0.09	0	-2	-1	0	2	0	-1
Mechanical Simplicity	0.19	0	-2	-3	-2	-2	-1	-3
Life-Cycle Cost	0.07	0	-1	-2	-1	-1	0	-1
Score		0	-0.39	-0.56	-0.11	-0.44	-0.12	-0.69
Rank		1	4	6	2	5	3	7

Based on the weights of the team's design drivers, the configuration selection process continued in comparing an SMR and a tandem rotor configuration. The mechanical simplicity and industry familiarity of the SMR configuration cannot be understated. It is the most widely used configuration and requires little to no extra training to be properly integrated into a shipboard environment. In addition, the tandem rotor configuration required two drive shafts, which is not a feasible configuration when dealing with a low GTOW and high payload weight.

Overall, the SMR design set a base for *Ibis'* simple, yet effective, design. Capable of completing both missions set forth by the RFP as well as countless others, *Ibis* is a versatile solution to current and future problems.

3 Vehicle Sizing and Aerodynamics

3.1 Size Restrictions

Many of the RFP requirements detail sizing restrictions. The takeoff and landing footprint, storage space, and payload volume were all specified. Taking each of these requirements into account, the main rotor was sized first based on the landing zone limits. Since the spatial accuracy was limited to 1m, the main rotor could not have a 6m diameter, leaving no room for error or an extended tail boom. Instead, a self-imposed restriction of 4x4m, as shown in Figure 14, was placed on the design to ensure *Ibis* fit comfortably into the landing zone, storage hangar, and would have no issue staying within the helipad bounds when landing. Figures 15 and 16 depict how *Ibis* fits in the takeoff and landing zone limits, and a maximum of 7 *Ibis* aircraft can fit in the hangar space.

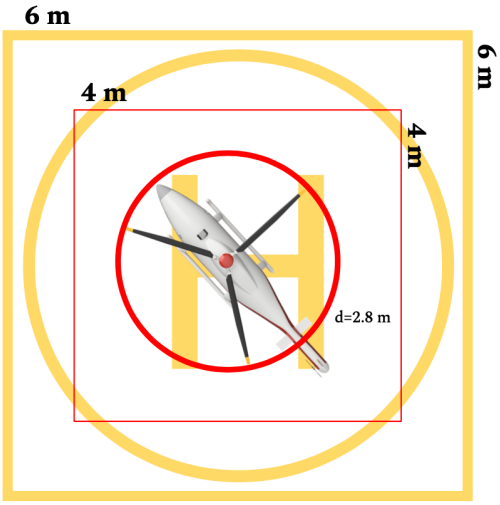

Fig 14: Sizing Restrictions on Main Rotor

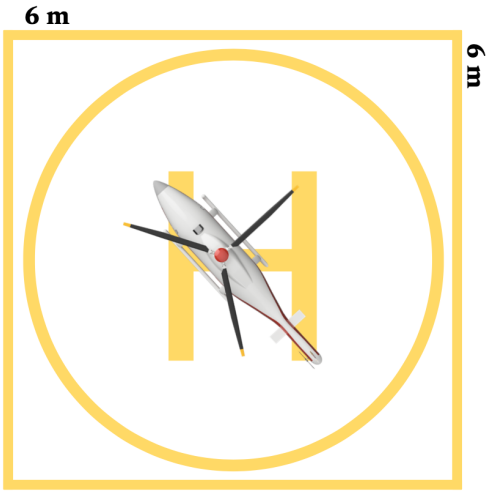

Fig 15: *Ibis* in Landing Zone

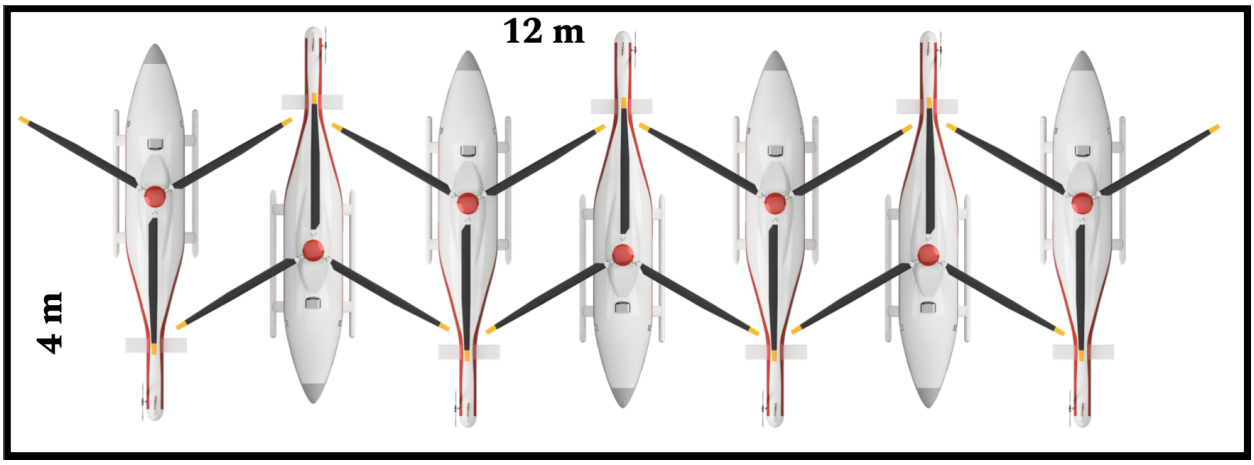

Fig 16: *Ibis* Storage Hangar

3.2 Methodology

The RFP lists two missions that *Ibis* must complete: a Supplies Delivery Mission and a Long Endurance communications relay mission. Neither mission holds precedence, and the vehicle must be capable of completing both missions with few modifications. This required determining an appropriate vehicle configuration for the design mission. An in-house sizing code was developed utilizing modified momentum theory to determine the power, speed, and fuel weight required for each segment of both missions, although a fixed forward speed was selected initially for simple analysis. The weights of each subsystem were estimated based upon equations outlined in the U.S. Army Aero Flight Dynamics Directorate (AFDD) presented in NASA Design and Analysis of Rotorcraft (NDARC) [3]. The engine and avionics subsystems were not estimated as both were selected from a study of commercially available options, however an early version of the sizing code estimated the engine weight. A flowchart of the iterative sizing procedure is shown in Figure 17.

An in-house MATLAB code based on the iterative procedure shown in the flowchart (Figure 17) was developed to carry out the initial sizing of the helicopter based on the mission requirements and user inputs. It begins with the specification of mission requirements, such as the payload weight, minimum cruise speed, and range of the helicopter. Tishchenko's method [4] was used to size the conventional single main rotor-tail rotor configurations. AFDD weights relations [3] were used to calculate the component weights. This procedure requires multiple iterations, and besides estimating the GTOW, it must also estimate flight speeds for each segment within the limits defined by the RFP.

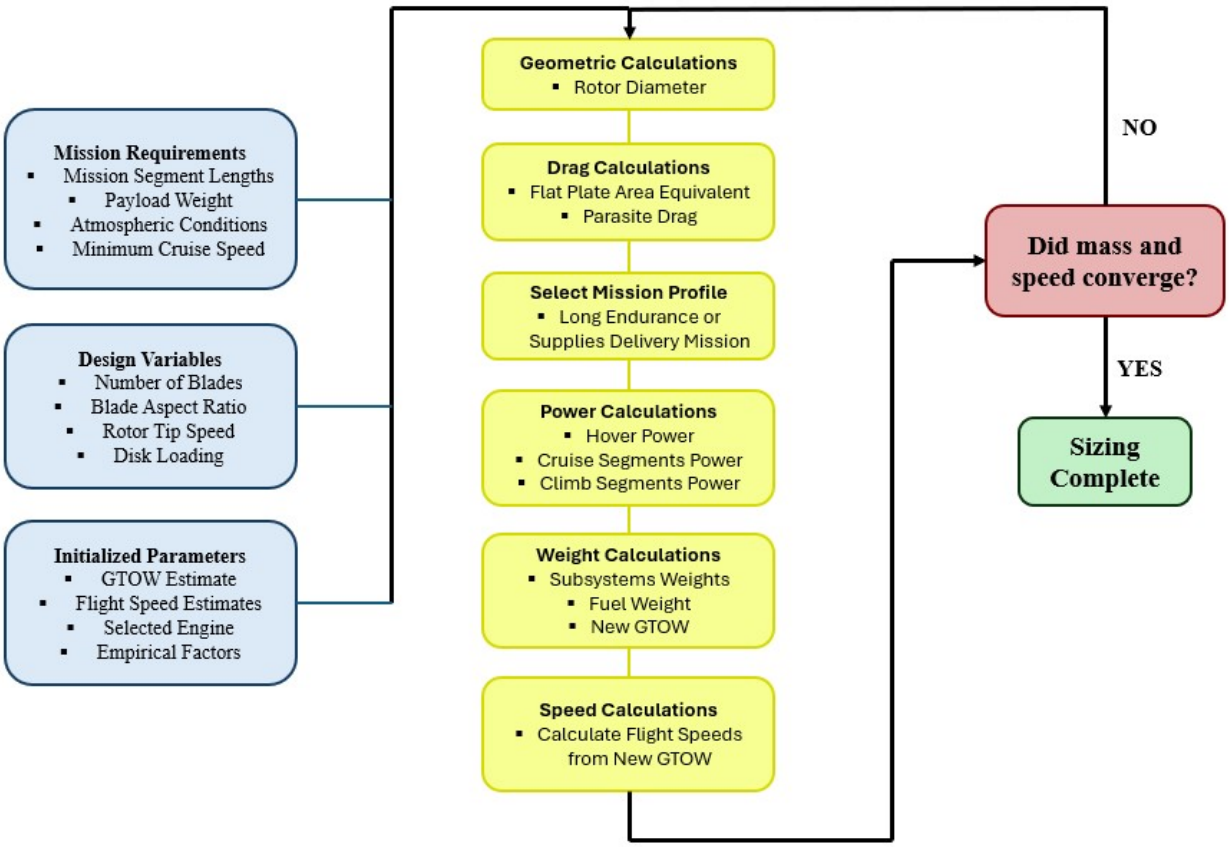

Fig 17: Flowchart of Sizing Code Procedure

3.3 Main Rotor Trade Studies

Initial main rotor analysis centered on the number of blades, as this parameter defines the type of rotor hub we would require. Maintaining constant aspect ratio and tip speed, 2, 3, and 4-bladed rotors were analyzed with variation in disk loading from 120 to 311 N/m^2 (2.5 to 6.5 lb/ft^2) to estimate the GTOW of the vehicle (Figure 18). At low disk loading, the weight of the vehicle increases as blade number increases. A 3-bladed rotor was selected for a low vehicle weight, moderate disk loading for a rotor diameter within storage hangar limits, and good gust tolerance.

Having selected a 3-bladed rotor for *Ibis*, the aspect ratio (solidity) and disk loading were varied to estimate the corresponding GTOW. The main rotor disk loading was varied from 120 to 311 N/m^2 (2.5 to 6.5 lb/ft^2) and solidity was varied from 0.04 to 0.06 (Figure 19). A blade aspect ratio of 23.4 (σ = 0.04) results in a small chord of 0.059 m (2.35 in) and small blade thickness of 0.007 m (0.28 in) which was deemed too difficult to manufacture and handle. Therefore, an aspect ratio of 19.1 (σ=0.05) was initially selected despite contributing to a heavier vehicle. To fulfill both mission requirements, a disk loading of 235 N/m^2 (4.9 lb/ft^2) with a rotor radius of 1.40 m (4.58 ft) was selected corresponding to a solidity of 0.05, and thus amounting to an estimated GTOW of 144 kg (317 lbs) for the rotor configuration. This configuration shows that the vehicle GTOW for both missions is the same. The rotor radius fits within the designated size restrictions of the landing footprint and storage space.

4 Main Rotor Design

4.1 Main Rotor Aerodynamic Design

The main rotor aerodynamic design was completed using an in-house Blade-Element Momentum Theory (BEMT) code for hover and forward flight to calculate the rotor performance in terms of figure of merit (FM) and lift-to-drag ratio (L/D) in cruise. The long endurance mission loiter segment was also examined for L/D as it comprises a large portion of the mission. The code was validated using flight test data of the R-66 helicopter. The main rotor

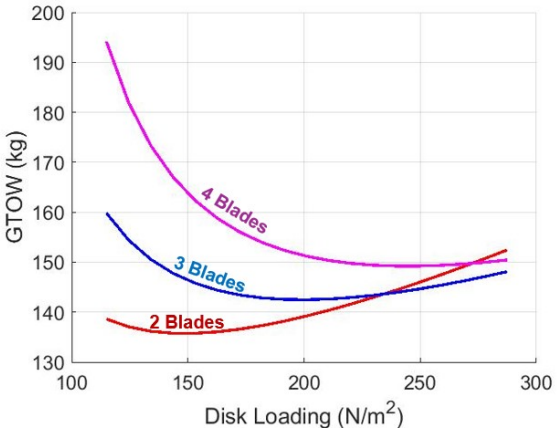

Fig 18: Gross Takeoff Weight Variation with Disk Loading for Main Rotors with 2, 3, and 4 Blades

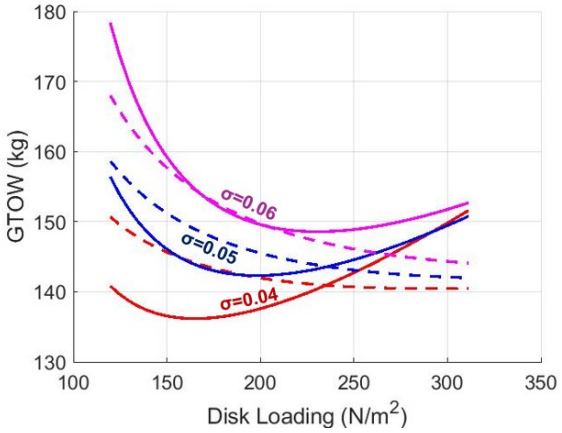

Fig 19: Gross Takeoff Weight Variation with Disk Loading for a 3-Bladed Main Rotor for Solidities of 0.04, 0.05, and 0.06

design aimed to maximize L/D as the rotor spends the majority of both missions in forward flight and reduce power consumption to reduce fuel usage.

The rotor blade design systematically examined various parameters: aspect ratio, airfoil, twist, taper, and tip speed. Multiple airfoils were not considered for geometric simplicity and easier manufacturability. Several airfoils were examined as shown in Figure 20: NACA0012, SC1095, RC4-10, RC3-8, OA209, SSCA09, VR15, VR12, and OA209. The OA212 airfoil provided the highest combination of FM in hover and L/D in forward flight. Blade aspect ratio was re-examined with BEMT to determine the aspect ratio that results in the highest L/D in cruise as shown in Figure 21. Reducing the aspect ratio of 19.1 (solidity of 0.05) selected from vehicle sizing to 17.05 (solidity of 0.056) lead to the highest L/D in cruise. Tip speed was set to 183 m/s (600 ft/s) to balance power consumption and blade loading considerations. Lower tip speeds produced higher FM as shown in Figure 22, but raised blade loading considerably. To limit blade stalling, the speed selected corresponds to a blade loading of 0.12 which maintains a FM above 0.8. An outboard taper ratio of 2 was selected to increase L/D while maintaining a sufficiently thick blade tip for simple manufacturing. The final blade design contains a bilinear taper and a single linear twist of -9.5°/span to reduce hover power. The complete set of design parameters are listed in Table 4.

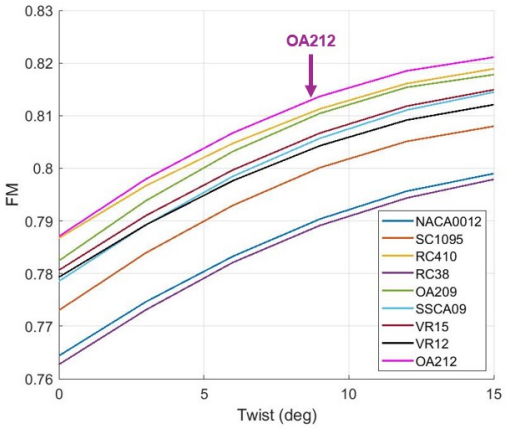

Fig 20: Airfoil Selection

Table 4: Main Rotor Design Details

Geometric Parameter	Value	Performance Parameter	Value
No.of Blades	3	**Disk Loading**	234.6 N/m^2 (4.9 lb/ft^2)
Aspect Ratio	17.05	L/D_{cruise}	5.23
Radius	1.40 m (4.58 ft)	L/D_{loiter}	4.12
V_{tip}	182.9 m/s (600 ft/s)	C_T/σ	0.12
Solidity, σ	0.056	**FM**	0.82
Main Rotor RPM	1251	$M_{tip}@V_{cruise}$	0.68
Power Loading, N/kW (lb/HP)	83.88 (14.05)	$\mu@V_{cruise}$	0.28

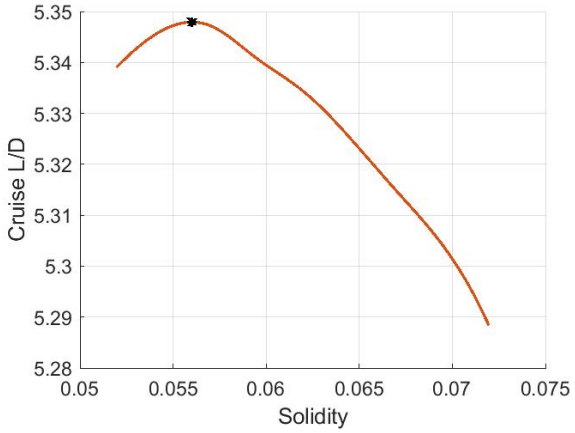

Fig 21: Solidity Selection

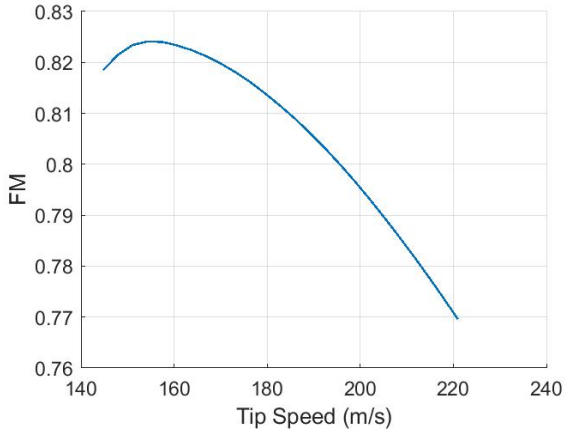

Fig 22: Tip Speed Selection

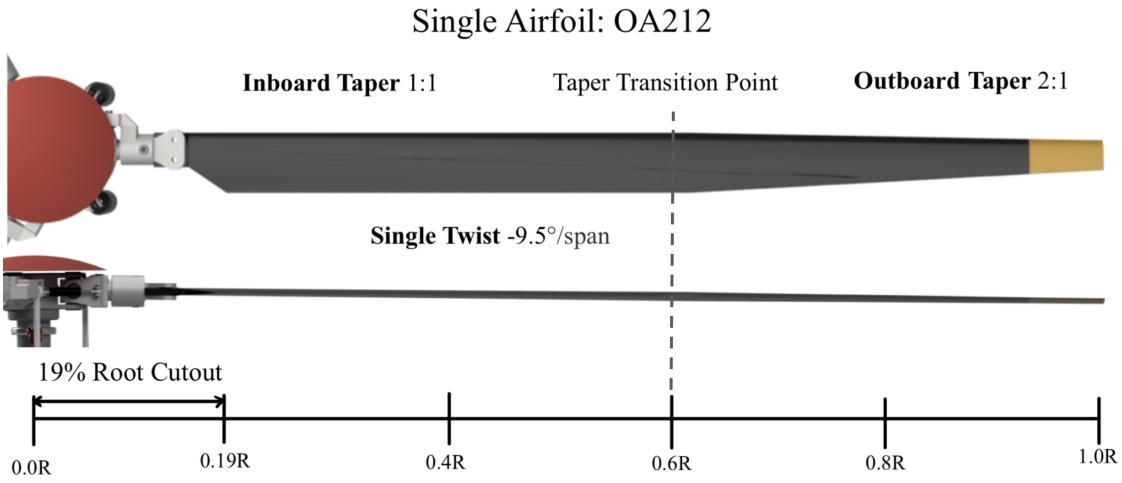

Fig 23: Main Rotor Blade Geometry

4.2 Main Rotor Blade Structure Design

The main rotor blade structural design prioritizes safety, reliability, and manufacturing simplicity. The structural composition of the blade is shown in Figure 24. The unidirectional carbon/epoxy D-spar is the primary load bearing component resisting centrifugal forces and flap and lag bending loads. The D-spar occupies the leading one-third chord length of the blade. This ensures the hub blade grip attachments fully insert into the D-spar. Torsional stiffness is provided by two layers of woven carbon-fiber fabric and epoxy laid in a $\pm$ 45° orientation. A glass-fiber epoxy trailing edge wedge provides additional lag bending stiffness to reduce the possibility of trailing edge delamination. To maintain the shape of the blade, Rohacell 51 foam fills the D-spar and Rohacell 31 foam fills the trailing two-thirds of the blade. A denser foam is used to shift the chordwise center of gravity forward. Tungsten leading edge weights shift the chordwise center of gravity to the quarter-chord position where the pitching axis is located to ensure aeroelastic stability. A thin copper mesh covers the blade skin to protect against lightning strikes that otherwise can severely damage the blades. A stainless steel erosion strip is placed at the leading edge to protect against abrasion due to sand, water, and other particulate matter.

4.3 Main Rotor Hub Selection

The main rotor hub is important in determining *Ibis'* vibratory loads, control characteristics, and stability. It transmits torque from the main rotor shaft to the blades, allows flap, lead lag, and pitch articulation and transmits control inputs to the rotor. Several hub configurations have been successfully demonstrated on helicopters in industry.

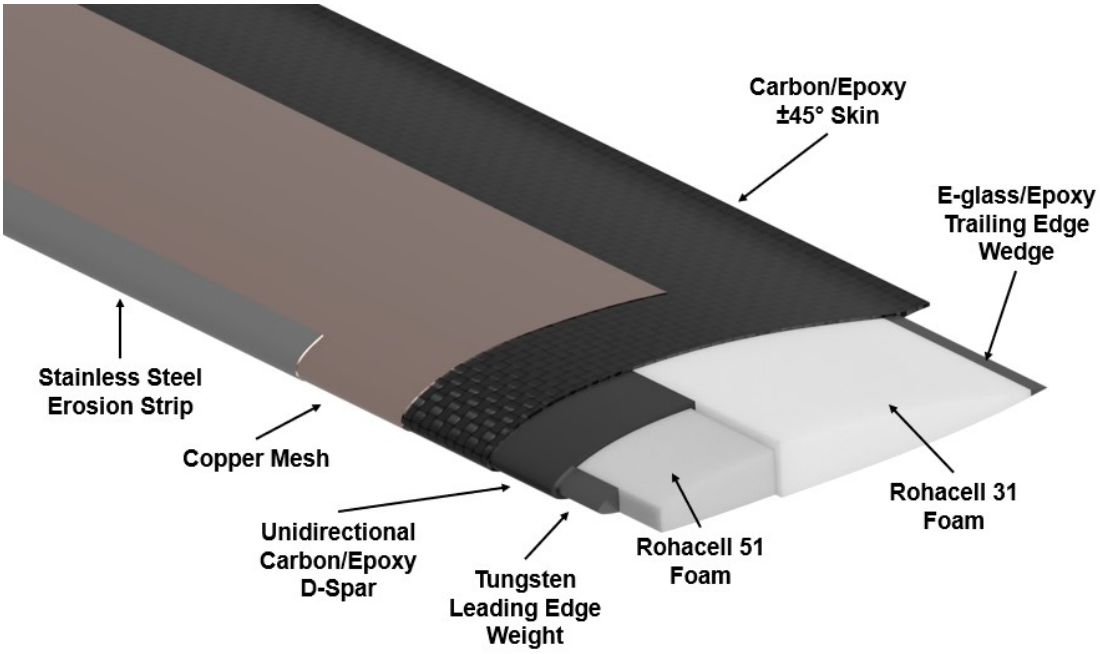

Fig 24: Blade Structural Composition

Aerodynamic analysis determined that *Ibis* would have 3-blades. Thus, the teetering hub was not considered. A trade study of 3 rotor hub configurations was conducted to select *Ibis'* main rotor hub: articulated, hingeless, bearingless.

A set of design drivers were considered to identify the best hub for *Ibis'* mission: mechanical complexity, gust sensitivity, controllability, weight, and manufacturing cost.

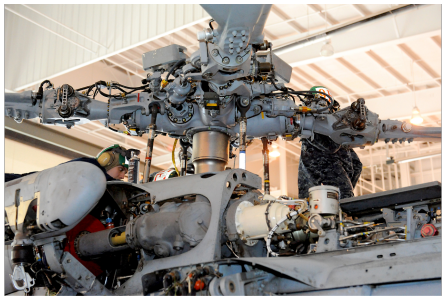

Fig 25: Sikorsky MH-60 Articulated Hub

Fig 26: Airbus H125 "Starflex" Hingeless Hub

Fig 27: Bell AH-1Y Bearingless Hub

4.3.1 Articulated

Articulated rotor hubs (Figure 25) utilize mechanical hinges for flap, lead lag, and pitch. This results in relatively low hub stresses, low vibrations, and gust insensitivity. However, articulated rotor hubs are heavy due to bearings and hinges in all 3 axes accounting for 6% to 7% of vehicle GTOW [4]. Furthermore, the mechanical hinges and bearings require regular maintenance. Articulated hubs generally have small flap hinge offsets, typically having a flap frequency of ∼1.04/rev and good rotorcraft controllability.

4.3.2 Hingeless

Hingeless rotor hubs (Figure 26) utilize innovative fiber composites to replace complex lead-lag and flap hinges with a single composite flexure. An elastomeric bearing is often used to provide pitch articulation. Hingeless hub designs are simple and compact, well controllable, and lightweight (3-4% of vehicle GTOW) [4]. These designs are often expensive to initially manufacture due to the complexity of the composite flexure. On the other hand, the lack of flap and lag mechanical hinges can result in lower maintenance requirements. Hingeless hubs typically have a higher flap frequency ∼1.1/rev. Thus, they have improved controllability due to quicker blade responses to control inputs. This higher flap frequency results in large blade bending moments, requiring additional blade maintenance inspections.

4.3.3 Bearingless

Bearingless hubs (Figure 27) do not have any mechanical hinges, instead using a single flex beam as a virtual hinge and bearing for all blade articulation. They are extremely simple as a single flex beam is the only component required for all 3 axes of articulation. However, the flex beam design and manufacturing is more involved. The flex beam is soft in torsion to allow for pitch articulation [4]. However, it still requires a wide torque cuff around the flex beam to lower pitch link loads, necessitating a large root cutout. Bearingless hubs come with the advantages of improved controllability from quicker blade responses to control inputs, limited servicing requirements, and light weight along with the disadvantage of greater vibrational issues. Flap frequencies of bearingless rotor hubs are normally lower than hingeless designs (∼1.05/rev). The single flex beam requires frequent inspection because it is subjected to high loads and strains in multiple directions.

4.3.4 Hub Configuration Selection

Ibis uses a fully articulated main rotor hub. Hingeless and bearingless hubs use elastomeric bearings that highly wear in the shipboard environment. Also, bearingless rotors are difficult to design, expensive to manufacture, and require elastomeric components. Articulated rotors can be made simpler using commercially available components, especially at *Ibis'* size scale. Thus, the articulated rotor was selected for *Ibis*.

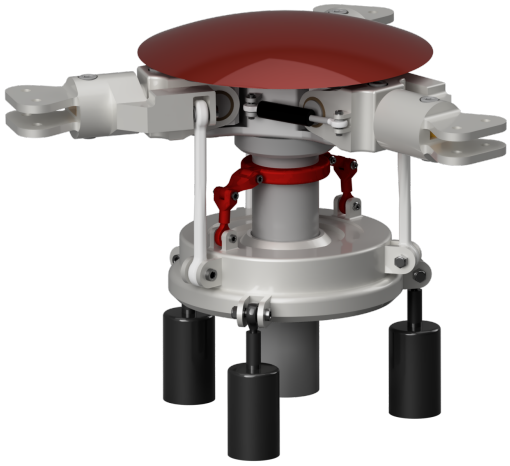

Fig 28: *Ibis* Main Rotor Hub and Swashplate

4.4 *Main Rotor Hub Structural Design*

Figure 28 shows the design of *Ibis'* 3-bladed articulated rotor hub. The design contains hinges for all three primary axes: flap, lead-lag, and pitch (Figure 29). *Ibis'* main rotor system is built around a lightweight aluminum yoke. A tension-torsion strap is housed in each blade grip for blade retention. The tension-torsion strap in *Ibis* is composed of two grooved bushings wound with Spectra fiber and enclosed in resin. This component carries tensile loads due to centrifugal forces and twisting due to rotor pitch control inputs. The main rotor system also features a sealed low-maintenance hydraulic lag damper. The rotor hub is designed to be lightweight and compact. Using the mass analysis tool in SolidWorks, *Ibis'* main rotor hub weighs only 6.7 kgs (14.8 lbs). Furthermore, the compact packaging of the rotor hub results in a 19% blade root cutout.

4.5 *Main Rotor Hub Dynamics*

Flap and lag hinges are coincident at 6% of the rotor radius. Using a rigid-blade blade model of the rotor system, the first non-dimensional flap and lag frequencies are estimated using equation 1 and equation 2, where $\bar{e}$ is the respective hinge offset divided by rotor radius. *Ibis* has a flap frequency of 1.047/rev and lag frequency of 0.31/rev. Because of the low in-plane frequency, a damper is included to mitigate ground resonance issues.

$$\nu_\beta^2 \approx 1 + \frac{3}{2} \cdot \frac{\bar{e}_\beta}{1 - \bar{e}_\beta} \tag{1}$$

$$\nu_\zeta^2 \approx \frac{3}{2} \cdot \frac{\bar{e}_\zeta}{1 - \bar{e}_\zeta} \tag{2}$$

Possible pitch-flap instability was avoided by having a high torsional frequency and blade chordwise center of gravity (CG) ahead of the quarter chord. Articulated rotors do not suffer from flap-lag instability. Also, articulated rotors do not suffer from air resonance [5]. Therefore, our rotor is free from aeroelastic instabilities. Based on the Deutsch stability criteria, and being equipped with a hydraulic lag damper, *Ibis* is free from ground resonance. *Ibis* uses an articulated rotor with low hinge offset and operates at a low advance-ratio which results in low vibratory loads. Therefore, there is no necessity to include vibration suppressors.

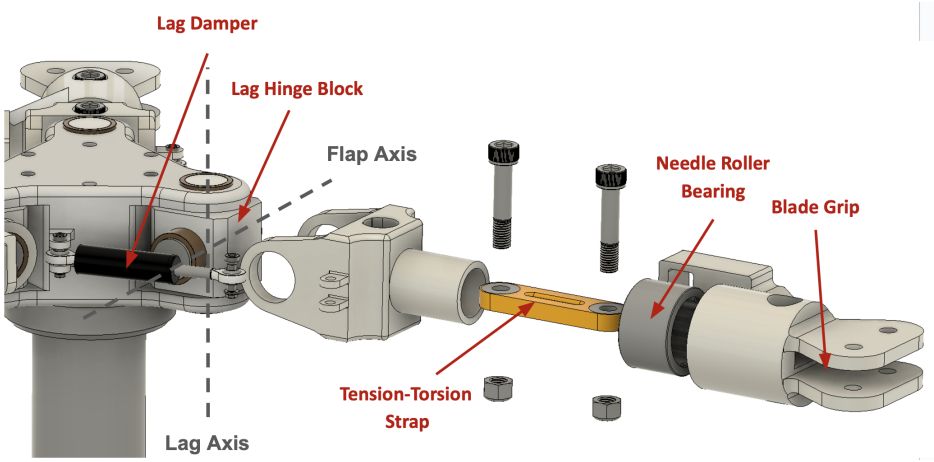

Fig 29: Main Rotor Hub Components

Control inputs are transferred to the rotor through a traditional swashplate (Figure 30). A swashplate is a mechanical device that transfers control inputs from the fixed frame to blade motion in the rotating frame by directly actuating a rotating disk linked to the blades. Cyclic and collective control inputs are effected by three high-bandwidth ball-screw based electromechanical actuators that actuate the lower swashplate. We are avoiding hydraulic actuation to minimize environmental impact of the vehicle.

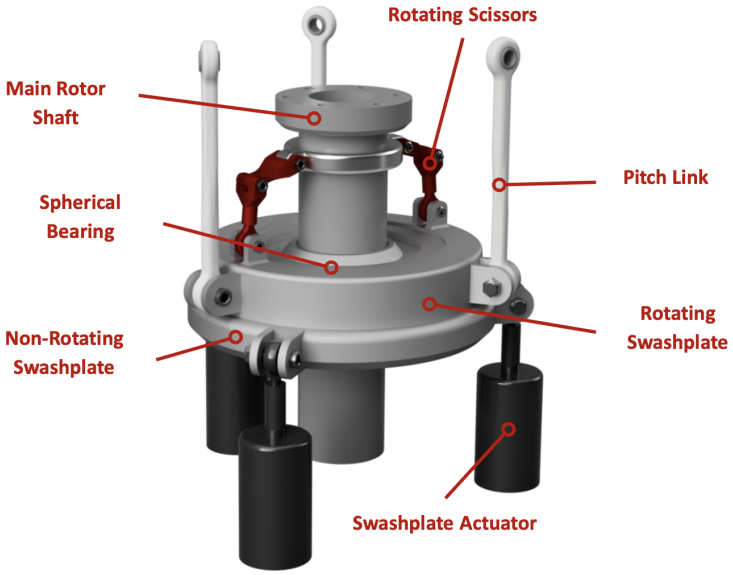

Fig 30: Swashplate Components

5 Tail Rotor and Empennage Design

5.1 Tail Rotor Aerodynamic Design

Tail rotor blade design followed the same procedure as the main rotor using an in-house BEMT code. The tail rotor was sized to provide sufficient thrust to counteract the torque generated by the main rotor. The tail rotor blade design prioritized a high FM as the vertical tail provides the majority of counter-torque in forward flight. For simplicity and to reduce forward flight drag, a 2-bladed tail rotor was selected with a radius of 0.27 m (0.89 ft) for the highest FM (Figure 32). Tip speed was set to be close to the main rotor tip speed while also ensuring that the gear teeth of intermediate gear boxes are prime factor ratios. A solidity of 0.094 (AR = 6.77) was selected as it results in the highest FM as shown in Figure 31. The blades have a linear twist of 10° to increase figure of merit further and no taper for simple manufacturing. The tail rotor parameters are listed in Table 5 and a complimentary diagram is presented in Figure 33. The tail rotor is positioned such that the blade tips are at minimum of 0.15 m (6 in) from the main rotor blade tips as specified in MIL-SPEC-8698 [6].

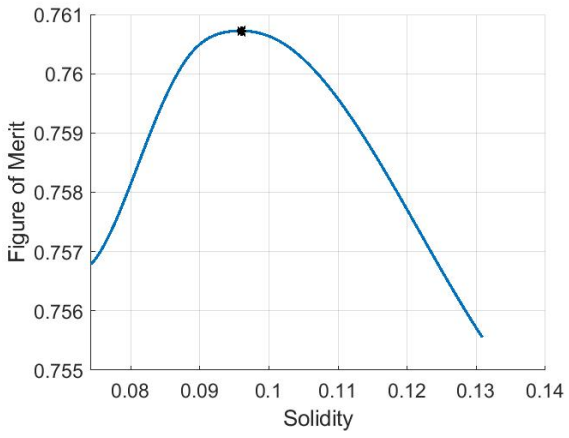

Fig 31: Tail Rotor FM vs Solidity

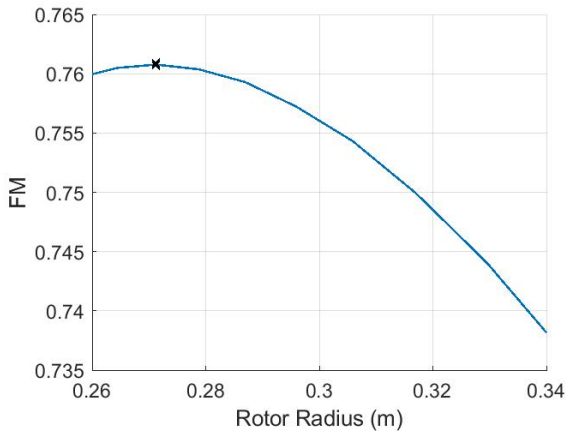

Fig 32: Tail Rotor FM vs Radius

Table 5: Tail Rotor Design Details

Geometric Parameter	Value	Performance Parameter	Value
No.of Blades	2	**Disk Loading**	38.08 kg/m^2 (7.80 lb/ft^2)
Aspect Ratio	6.77	**Tail Rotor RPM**	6760
Radius	0.271 m (0.89 ft)	C_T/σ	0.093
V_{tip}	192.0 m/s (630 ft/s)	**FM**	0.765
Solidity, σ	0.094	$M_{tip}@V_{cruise}$	0.71

Fig 33: Tail Rotor Blade Geometry

5.2 *Tail Rotor Hub Structural Design*

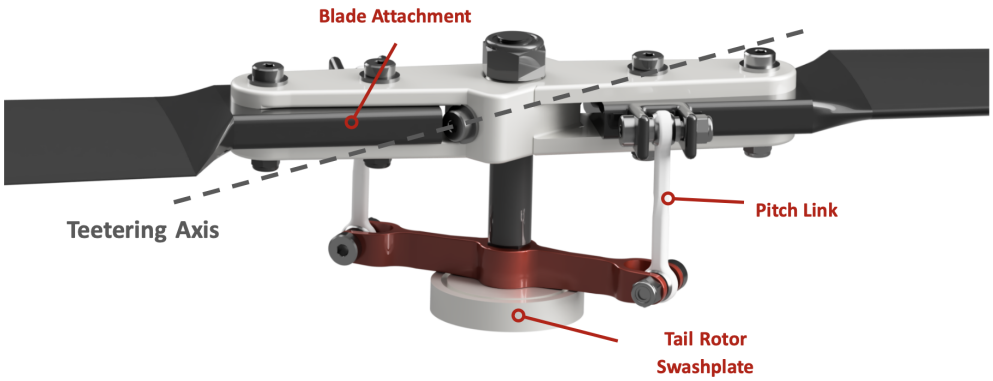

Fig 34: Tail Rotor Hub

The tail rotor hub and actuation is designed with simplicity in mind. Thus, the proven design of a teetering hub was used. Collective control is actuated by a swashplate collocated on the tail rotor shaft. 45° of δ_3 was included to reduce tail rotor flapping as recommended in U.S. Army Air Mobility Research and Development Laboratory (USAAMRDL) Technical Report 73-99 [7]. The tail rotor is positioned port side in the pusher orientation and rotates bottom forward to minimize power usage [7].

5.3 *Vertical Stabilizer*

A low drag NACA4412 airfoil was selected for the vertical stabilizer. The tail rotor gearbox is placed in the tail boom, so a thin airfoil could be used. Positioned at an angle of 6° to provide the highest L/D, a planform area of 0.0328 m^2 (0.35 ft^2) is required to counteract the main rotor torque of 87.09 N-m (64.24 lb-ft) in the return cruise flight (segment 10 in Figure 2 and segment 6 in 3). This planform area does not provide excessive anti-torque in the cruise flight to the destination (segment 4 of Figures 2 and 3) and loiter (segment 5 of Figures 2 and 3), maintaining a positive tail rotor collective throughout both missions. The vertical stabilizer is positioned above the tail boom to be closer in line with the main rotor. The vertical stabilizer is shown in Figure 35.

5.4 *Horizontal Stabilizer*

The primary purpose of the horizontal tail is to maintain pitch stability and counteract the fuselage pitching moment during cruise. *Ibis'* horizontal tail was sized by empirical data [4] based upon Eqn. 3. The planform area of the horizontal tail is 0.0526 m^2 (0.567 ft^2). A NACA4412 airfoil was selected to provide sufficient lift at a low angle of attack while reducing drag. The horizontal stabilizer is placed 0.15m (6 in) ahead of the tail rotor blade tips in compliance with MIL-SPEC-8698 [6]. The horizontal stabilizer is shown in Figure 35.

$$S = 0.0086 * \pi * R_{MR}^2 \tag{3}$$

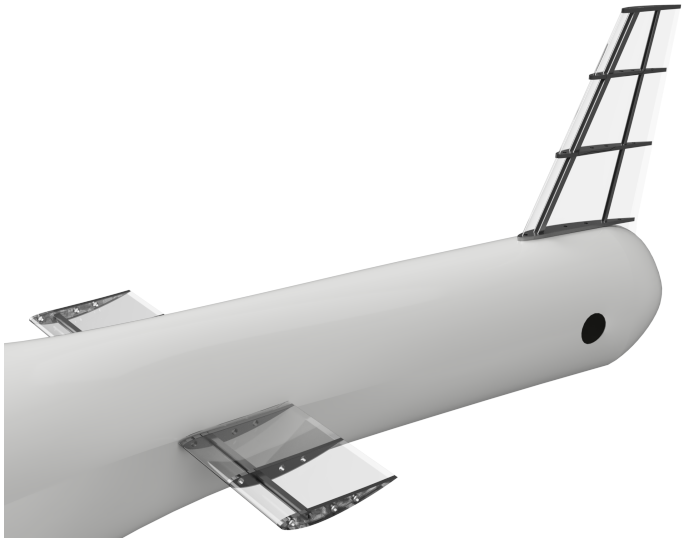

Fig 35: Empennage Configuration

5.5 *Flight Dynamics*

The horizontal tail contributes significantly to longitudinal stability. An inverted horizontal tail provides negative lift in forward flight to maintain pitch stability. An in-house UMD flight dynamics modeling and simulations code was used to analyze *Ibis'* flight stability. A slightly unstable phugoid mode root was identified, and therefore, the aircraft requires a stability augmentation system.

6 Propulsion and Transmission Design

6.1 *RFP Requirements*

The RFP requirements for propulsion and transmission systems state that power generation must produce either zero emissions, or run on Jet-A fuel. Auxiliary power needs to be provided at 800 Watts for the long endurance mission and 400 Watts for the supply delivery mission. This means that the engine needs to generate rotational energy in the

rotor and electrical energy for the avionics. To do this the design must either use a battery and electric motors, an engine and an alternator, or some combination of the two.

6.2 Power Generation

Based on performance estimates (reported in Section 10.4), the engine needs to supply at least 27 kW (36.5 hp) directly to the rotor during vertical take-off. Accounting for emergency power needs that may arise in less favorable conditions, the design should be able to generate extra power. Rounding up to account for a slight margin of error means that the engine or battery needs to be capable of providing a steady 30 kW (40 hp).

6.2.1 Battery Trade Study

A quick calculation rules out using a battery as an energy source. As an example, assume that for cruise the helicopter only needs 15 kW (20 hp). For a 3-hour cruise, the total energy required is 45 kWh. Table 6 shows some available batteries and their energy densities. At 45 kWh, a lithium-ion battery at 165 Watt-hours per kilogram, the battery required would weigh 272 kg (600 lbs). The battery weight alone is over the 160 kg limit for GTOW. The cost would also be an issue because, at an average of about $3 per gram of lithium, of which 9,900 grams (150 grams per kilowatt hour) is required, the battery would cost $29,700. This consideration rules out lithium-ion batteries as a potential power source.

Table 6: Various Batteries' Energy to Weight Ratio

	Energy Density Wh/kg
Lead Acid	30
Lithium-Phosphate	120
Lithium-Cobalt	150
Lithium-Ion	200
Lithium-Manganese	700 [8]
Maximum Theoretical Specific Energy	1200 [9]

6.2.2 Turboshaft vs Piston Engines

Two groups of direct drive engines considered in our design: turboshafts and piston-driven internal combustion. Turboshafts are often more complex but have better power-to-weight ratios than their piston-driven counterparts. Internal combustion engines generally have lower fuel consumption and produce less noise, but often come with less altitude performance and stronger vibrations. The most relevant values are compared in Table 7.

Table 7: Turboshaft vs Piston Comparison

	Turboshafts*	Piston engines**
Power density kW/kg (hp/lb)	2.5 (1.5)	1.8 (1.1)
SFC g/kW-hr (lb/(hp-hr))	304 (0.5-0.6)	243 (0.4)
Noise Level	110 dB	70dB

*Estimates based on data from turboshafts in Table 8
**Based on the Deltahawk engine

6.3 Turboshafts

Based upon publicly available data, shown in Table 8, small turboshaft engines are in a developing stage. Companies have shifted their interest towards the production of small turboshafts for Class 3 UASs with GTOW $<$ 598 kg (1320 lb). As the design requirements put *Ibis* in the category of Class 3 UAS, there is a lot of emerging markets and potential growth to be made. From the data collected, however, current turboshafts are either rated for lower than 11 kW (15 hp) or higher than 75kW (100 hp). The max continuous power required for *Ibis* is 21.2 kW (30 hp).

Table 8: Turboshaft Engine Comparisons

	Jakadofsky [10]	PBS [11]	Turbaero [12]	Stuttgart Engineering [13]		Papiz turbines [14]	UAV turbines [15]
	Pro X	PBS TS100	TP200	STV100	STV130	Prometeo	UTPR50
Weight kg (lbs)	3.3 (7.28)	61.3 (135.14)	123 (271.17)*	28 (61.73)	30 (66.14)	50 (110.23)	31.75 (70)
TO Power kW (hp)	10 (13.41)	179.71 (241)	149.14 (200)	74.57 (100)	96.94 (130)	74.57 (100)	37.29 (50)
Max. continuous power kW (hp)		159.58 (214)	142 (190)				
SFC g/kW/hr (lb/hp/hr)	0.9072 (1.491)	0.548 (0.9009)	0.3467 (0.57)	0.3621 (0.5953)	0.3301 (0.5427)	0.2816 (0.4629)	0.3041 (0.5)
Dimensions m (ft) (diameter*length)	0.141*0.3 (0.436*0.984)	0.33*0.829 (1.083*2.720)	0.506*1.017 (1.66*3.337)	0.28*0.555 (0.919*1.821)	0.28*0.555 (0.919*1.821)	0.2*0.7 (0.656*2.297)	0.292*0.533 (0.958*1.745)
Fuel	Jet-A	Jet-A	Jet-A	Diesel	Diesel	Jet-A	Jet-A
TO power/Weight kW/kg (hp/lb)	3 (1.842)	2.932 (1.783)		2.663 (1.62)	3.23 (1.966)	1.49 (0.907)	1.17 (0.715)

* No dry weight data available, only Installed weight

6.4 *Turbogenerators*

An advantage of a turbogenerator compared to a turboshaft is eliminating the need for a shaft reducing weight. However, a turbogenerator will be heavier than a power-equivalent turboshaft, due to the presence of the generator. Some turbo generators are shown in Table 9.

Table 9: Turbogenerator Comparisons

	Turbotech		Honeywell	
	Tg-r55 X	Tg-r90	HGT1700	HTS900
Weight kg (lb)	55 (121.25)	64 (141.096)	460 (1014.13)	300 (661.39)
Takeoff Power kW (hp)	55 (73.76)	90 (120.69)	1000 (1341)	400 (536.4)
Max. Continuous Power kW (hp)			900 (1206.92)	
SFC g/kW/h (lb/hp/h)	0.548 (0.9009)	0.3467 (0.57)		
Fuel	Jet-A	Jet-A		

The Turbotech Tg-r55 X engine appears to be a likely canidate for our design. However, a further examination of the values obtained showed that installing a version of Turbotech's turbogenerator would not be a sensible option, due to an excessive weight penalty. The high weight of Turbotech's turbogenerators is likely because they are in an early development stage, and their power density can be expected to improve in the following years. These results leave the option of mounting a turboshaft with a separately manufactured alternator as the only feasible option.

6.5 *Final Engine Selection*

To best meet our needs, the UTP-50R from UAV Turbines was selected for power production. Their next generation, the Monarch V engine, may be better suited for our needs once it finally reaches production. However, it is currently in testing at a much lower Technology Readiness Level and is outside of the 5-year development limit.

The UTP-50R is a micro-turbine that generates more power without many downsides when compared to other turboshaft engines around the same power output (Table 8). The main draw to their design is the recirculation of exhaust heat. To improve the energy captured by the turbine, exhaust gas is pumped through a heat exchanger just after combustion to recapture the excess heat. This helps to mitigate the losses from blade leakage that happens inside every turbine-driven engine. This also acts to further cool the outside of the engine as well as the exhaust gas. This makes complying with AR56-3.1.1.8 [6] easier as there is less waste heat to manage.

The mounting is shown in Figure 36, with rubber dampers pinning the engine in place and additional space for airflow to cool the externals complying with AR56-3.1.1.8 [6] and 3.6.5.2 [6]. Conforming with AR56-3.6.4 [6], the engine operates at 107,000 RPM (converted to 6000 RPM through the nose gearbox), so the resonance between the engine, transmission, and main rotor is non-existent. A ring mount was added just behind the nose gearbox to provide

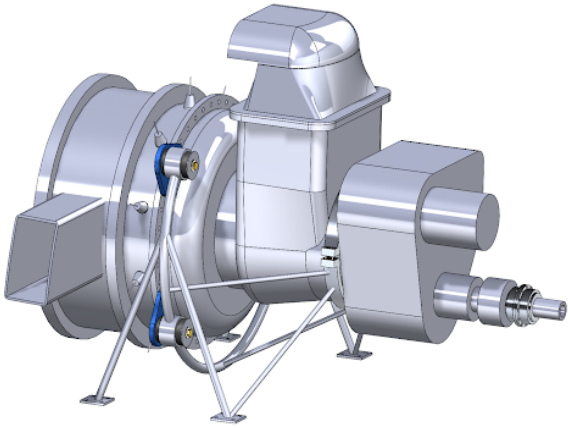

Fig 36: UAV Turbine's UTP 50R Engine

extra support during some high-g maneuvers. Additionally, the noise level complies with AR56-3.6.6 [6], due to high-frequency noise produced attenuating quickly in the air.

6.6 *Fuel Management*

The fuel system is made up of three tanks; one 38 liter (10 gal) tank placed above the keel beams and close to the tail boom, one 22.7 liter (6 gal) tank placed above the keel beams and close to the nose cone, and one 0.343 liter (0.1 gal) collector tank placed on the transmission deck just below the engine intake. To minimize sloshing and internal movement of the fuel as the tanks empty, baffles are placed inside the two larger tanks. The tanks are connected as shown in Figure 37.

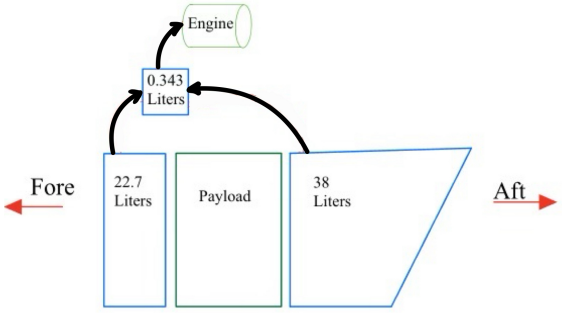

Fig 37: Fuel Tank System

Fig 38: Fuel Tank Door Access

The tanks (shown as the yellow boxes in Figure 38) are easily accessible via the payload door on the port side of the vehicle. During the long endurance mission, when all three tanks are in use, the 22.7 liter front tank will be fully burned through before utilizing the fuel in the 38 liter tank in order to minimize the movement of the center of gravity (CG). The front tank is able to be removed as a module add-on, which is detailed further in Section 8.2.

6.7 *Transmission and Gearbox Design*

For the UTP50R engine, the nose gearbox reduces the turbine speed of 107,000 RPM to an output speed of 6000 RPM, and the rotor is designed to rotate at 1250 RPM. This means the gearbox will need to be stepped down by a factor of 4.8 to 1. This reduction could be achieved by a single stage, however, for the clearance needed to run the tail drive shaft, another reduction is used to split the transmission for the tail and main rotor sections. This elevation is achieved with a V-belt since a gear at this size would be far too large and require extra lubrication. At the tail, a bevel gear increases the speed from 6000 RPM to 6800 RPM.

A double drive-belt system, similar to the one used on the Robinson R-22 (shown in Figure 40), was mounted for the first reduction. The double belt was chosen over a set of gears for weight reduction and the additional clearance.

Two V-shape belts, selected due to their reliability and redundancy, transmit the torque to the bevel gear. In the event of failure of one of the belts, the engine could still transfer power to the main rotor and land safely. In addition, the engine shaft connects directly to the tail rotor; in case of failure of both belts, the *Ibis* could still autorotate safely.

The high RPM means that any instability or imbalance in the gearbox or engine will result in high-frequency vibrations. These vibrations would erode any bolts or pins that would hold it rigidly, so a softer material is needed to dampen the impact. AR56-3.6.5 [6], requires that every part that maintains sufficient vibrations is mounted with dampers similar to that on the gearbox on the Robinson helicopters seen in Figure 39.

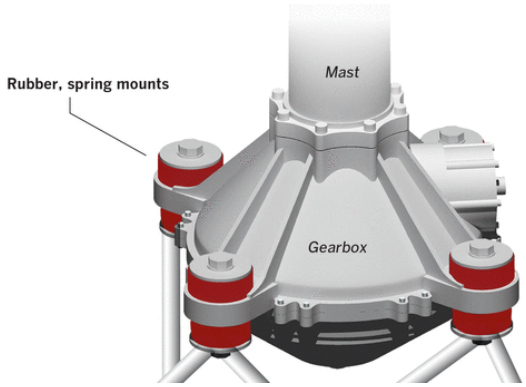

Fig 39: R44 Gearbox Dampers

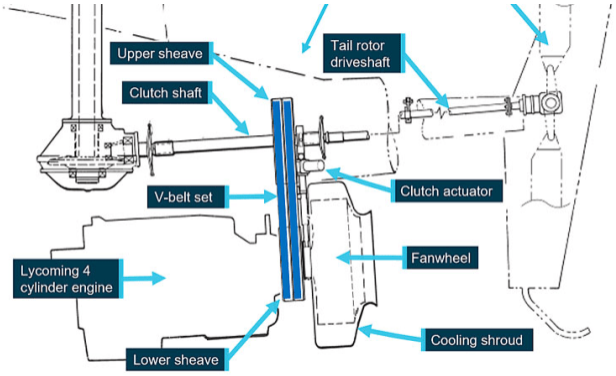

Fig 40: R22 Double Belt-drive system

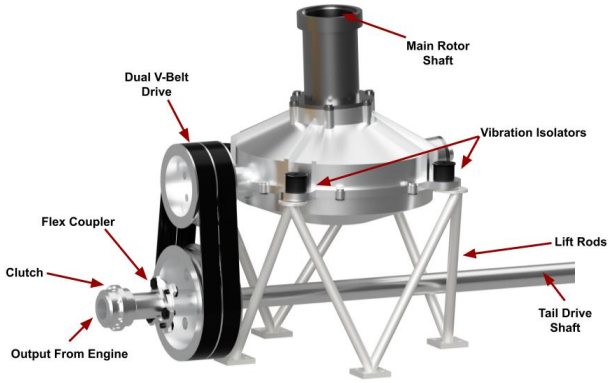

Fig 41: R44 Gearbox Dampers

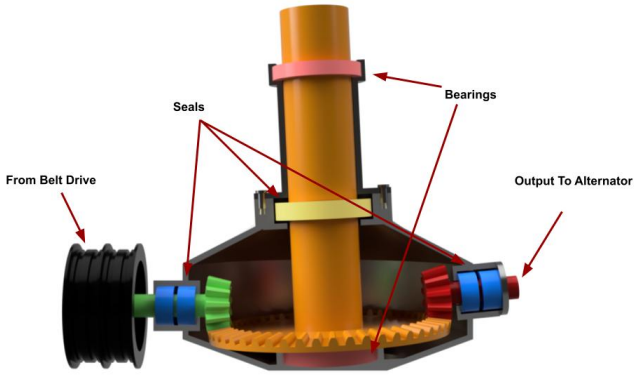

Fig 42: Main Gearbox Internals

Flex couplings allow for minor misalignment caused by bending that the aircraft might experience due to the applied loads. The tail and engine portions are largely susceptible as they will have large moment arms and can result in misalignment in the shaft. There is a flex coupler between the engine and main gearbox, and two along the tail drive shaft.

The alternator requirements are very standard so the AL12-F70 Hartzel Plane Alternator was selected as it is capable of generating the needed 800 Watts for the power bus. Its lightweight, reliable, as well as FAA PMA Certified to be operated in general aviation applications.

The final design for the main rotor gearbox is shown in Figure 41. The gears are made of high-strength steel. They are well lubricated which protects them from wear. Based on the relatively high gear ratio, the gears have a hardness of Rockwell C 38-63. The main rotor mast casing will be made of cast aluminum as it will experience the highest loads and is the central force driving the helicopter. This also makes it resistant to marine corrosion.

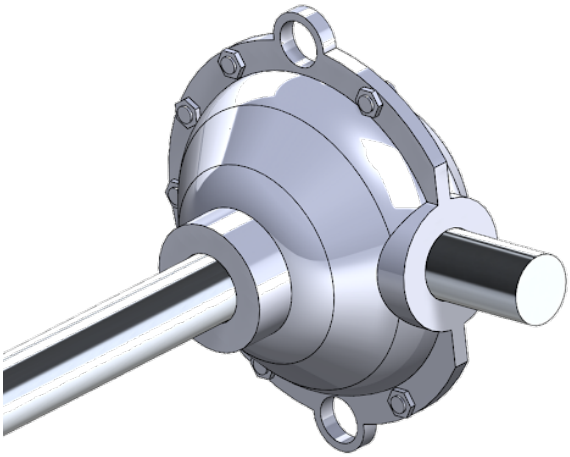

Fig 43: Tail Gearbox

7 Structural Design

When designing the airframe structure, the important characteristics are the weight, structural integrity, and payload design/handling. These topics are addressed in this chapter.

7.1 Material Selection

Preferable characteristics for materials include corrosion resistance, high strength-to-weight ratio, and durability. Some materials such as steel, aluminum, and titanium as well as composite materials (carbon fiber and glass fiber) were studied. Materials are listed in Table 10 with pros and cons for each type of material.

Table 11 shows a comparative evaluation of candidate materials. A mixture of aluminum alloys and composite materials was selected due to aluminum's effectiveness against seawater corrosion and light structural weight as well as composite material's lightweight. Table 12 provides the density (ρ), Young's modulus (E), yield strength (σ_y), and ultimate tensile strength (σ_t) for *Aluminum 2024-T361* and *Toray T700S Carbon Fiber*. Lightweight and corrosion resistance were weighted the highest because *Ibis* operates in the maritime environment. Composites ranked first, aluminum alloy second, titanium alloy third, and steel alloy fourth. MIL-C-21180 and MIL-HDBK-17 were used to obtain the properties of these materials to meet army specifications and requirements for high-strength aluminum alloys and composites.

The fuselage bulkheads and landing gear are composed of aluminum alloy. The longerons are composed of composite material as it reduces the weight of the fuselage. To combat the composite material's relatively poor resistance against seawater corrosion, the vehicle components use these materials coated in paint and primer. However, there are many techniques to improve resistance against corrosion like, "...Electrochemical anodizing, thermal oxidation, chemical oxidation and bulk treatments such as alloying" [16]. For prevention of galvanization and seawater corrosion, the fuselage uses an Epoxy primer and Polyester urethane topcoat as they both meet MIL-PRF-23377F and MIL-PRF-85285E specifications respectively.

7.2 Landing Gear Design

Different landing gear configurations on Table 13 show the relative advantages and disadvantages of these concepts for *Ibis*. A fixed skid landing gear was chosen due to its lightweight. In order to ensure aerodynamic efficiency, elliptical cross tubes were used in the landing gear.

Table 10: Fuselage Material Pros and Cons

Materials	**Pros**	**Cons**
Steel Alloy	* High yield stress * High Young's modulus * Inexpensive and easy manufacturing process * Great for high-loading applications (i.e. landing gear)	* Relatively poor against seawater corrosion * Heaviest material * Low fatigue resistance
Aluminum Alloy	* Great against seawater corrosion * Light material * Inexpensive and easy manufacturing process * Inexpensive to purchase	* Low Young's modulus * Low yield stress * No fatigue resistance
Titanium Alloy	* Great against seawater corrosion * Highest strength to density for all metal alloys * Highest fatigue resistance * High-temperature resistance	* Difficult to weld or mechanically manipulate * Expensive material
Composite	* Highest strength to density for all materials * Lightest suggested material * Highest fatigue resistance	* Relatively poor against seawater corrosion * Expensive material * No deformation or explosive failure * Difficult to manufacture

Table 11: Analytical Hierarchy Process for Materials

	Corrosion Resistance		Lightweight		Durability		Cost		
	Weight	Score	Weight	Score	Weight	Score	Weight	Score	Final Score
Aluminum Alloy	0.21	0.39	0.51	0.24	0.20	0.07	0.09	0.64	0.27
Steel Alloy	0.21	0.15	0.51	0.12	0.20	0.42	0.09	0.17	0.19
Titanium Alloy	0.21	0.78	0.51	0.03	0.20	0.39	0.09	0.13	0.27
Composites	0.21	0.06	0.51	0.61	0.20	0.13	0.09	0.06	0.35

Table 12: Properties for Al 2024-T361 and Toray T700S Carbon Fiber

Materials	**AL 2024-T361**	**Toray T700S Carbon Fiber**
$\rho - \frac{kg}{m^3}\ \left(\frac{lb}{ft^3}\right)$	2780 (173.55)	1800 (112.32)
E - GPa (Msi)	72.4 (10.5)	230 (33.58)
σ_y - MPa (Ksi)	395 (57.29)	N/A
σ_t - MPa (Ksi)	495 (71.79)	4900 (711)

Table 13: Pros and Cons of Landing Gear Types

Landing Gear Type:	Retractable Wheel Landing Gear	Skid Landing Gear
Pros	* Easy to maneuver on the ground Enable running take-offs Potentially taking off with extra payload * Retracted, more streamlined	* Lightweight * Inexpensive manufacture/maintenance
Cons	* Extra weight and cost * Higher maintenance	* Cannot taxi on their own * Not easy to retract * Source of drag for forward flight

7.3 Stability

A sleeve with bolts, nuts, and washers is used to secure the *Ibis'* landing gear to the fuselage bulkheads as shown in Figure 44. Within the sleeve, there is fiberglass between the bulkhead connector and the landing gear in order to prevent galvanic corrosion.

Pitch and roll static landing gear stability is ensured when the tip-over angle is below 60°for pitch and 30°for roll [4]. Using *Ibis'* complete 3D model and component weights, the landing gear has an estimated pitch tip-over angle of 54.74°and roll tip-over angle of 28.11°(Figure 45). Thus, *Ibis* is statically stable.

The landing gear must sustain loads that occur during rough ship landings. The landing gear must be able to withstand an impact at 3.66 m/s (12 ft/s) with the rotor supporting 100% of the aircraft's weight [6]. The aircraft structure is designed to withstand 3.5g during flight as required in AR-56 [6]. Thus, the landing gear effectively must withstand a limited impact acceleration of 2.5g. The landing gear was analyzed using Chernoff's method [17].

To analyze the energy that the landing gear absorbs, first a load versus deflection curve for a specific landing gear tube thickness is made (Figure 46). The landing gear deflection for a given load was predicted using Autodesk Fusion360 FEA tools (Figure 47). The energy absorbed by the landing gear is calculated as the area under the load vs. deflection curve. This absorbed energy is equivalent to the kinetic energy due to a landing impact at 3.66 m/s (12 ft/s).

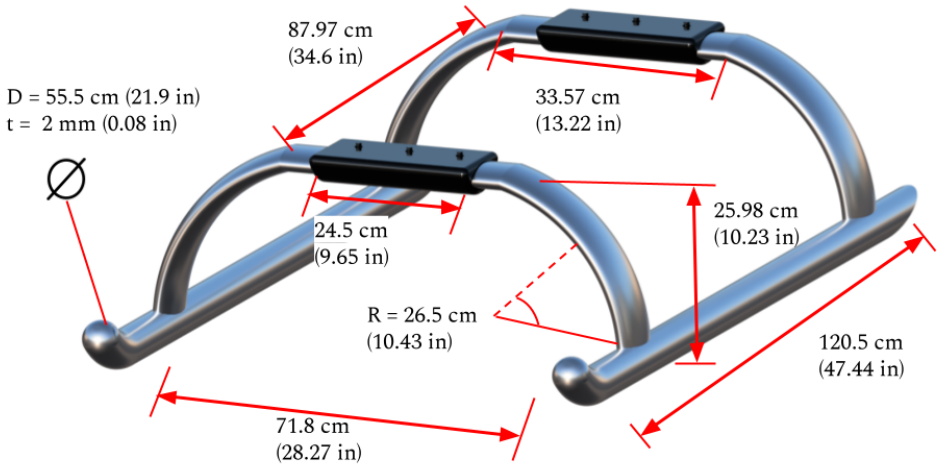

Fig 44: Landing Gear

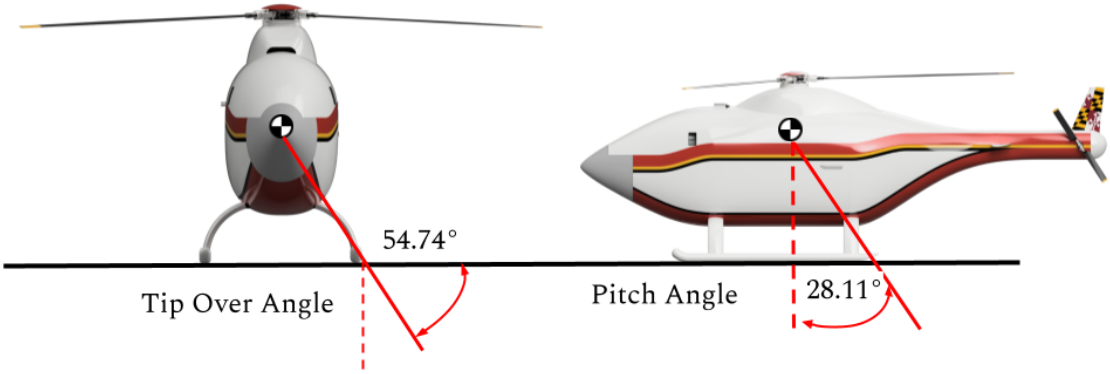

Fig 45: Landing Gear Stability Angles

The tube thickness was iterated until a thickness was found with an appropriate safety factor. *Ibis'* landing gear has a factor of safety of 3.16.

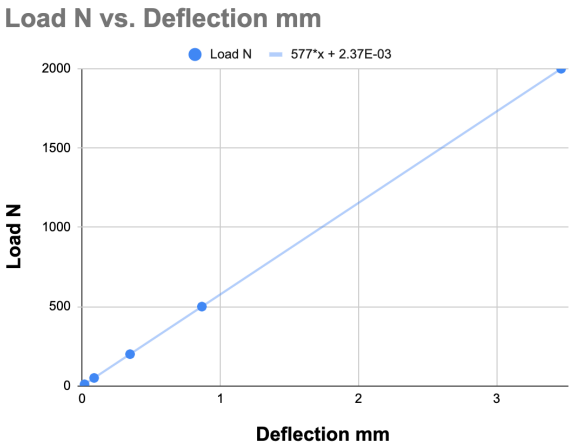

Fig 46: Load (N) vs Deflection (mm) Curve

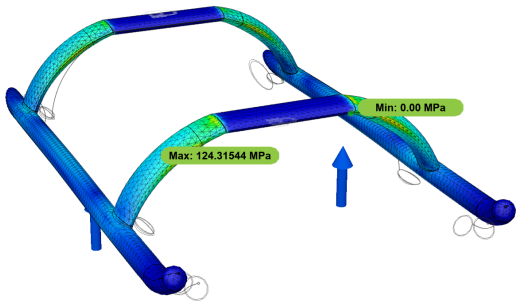

Fig 47: Stress Analysis of Landing Gear

7.4 Load Paths

When *Ibis* lands, loads from the landing gear are directly transferred to the central bulkheads. The loads will travel along the longerons and keel beams. When the helicopter is in flight, the vehicle will primarily experience loads from the rotor that get transferred to a steel reinforced portion of the gearbox and finally to the bulkheads and longerons. *Ibis'* internal structural design is shown in Figure 48.

7.5 Fuselage Trade Study

Circular, square, and super-ellipse fuselage cross sections were considered. Based on coefficient of lift graphs published by Adakuma et al. [18], square cross-sections generate more lift, are more aerodynamically efficient, and

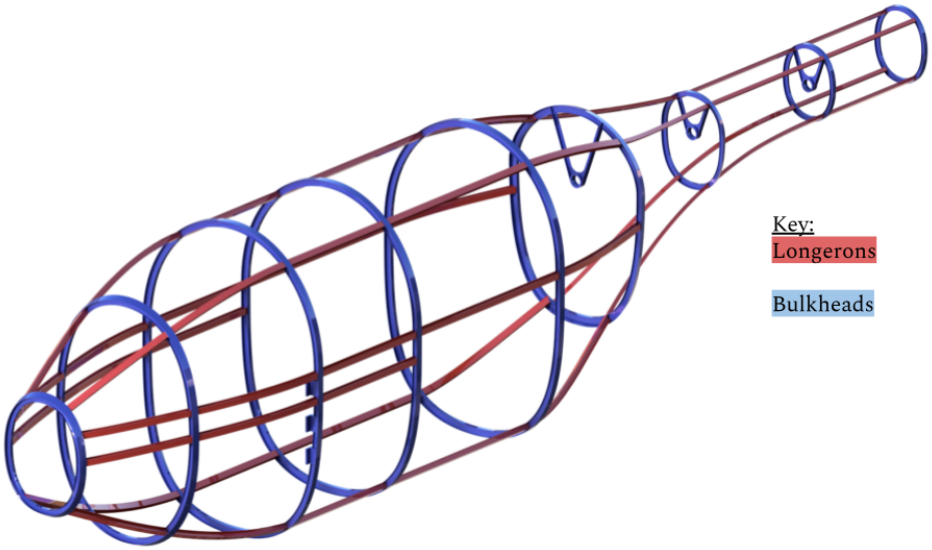

Fig 48: Finalized Fuselage Skeleton

Table 14: Trade Study on Fuselage Designs

Cross Section:	Super-Ellipsis	Square	Circular
Beneficial Qualities	*High L/D ratio *High Stability	*High L/D ratio *Larger Capacity	*Medium Stability *Easy to manufacture
Drawbacks	*Constrictive Capacity	*Difficult to manufacture	*Lower L/D ratio

have better lift-to-drag ratios than circular-cross sections. The super-ellipsis shape was also analyzed for its benefits and drawbacks. Figat et al. showed higher lift coefficients and increased stability of super ellipse cross-sections compared to a circular cross-sections [19]. A trade study was conducted based on this existing research in order to investigate the benefits and drawbacks of each shape in Table 14. *Ibis'* fuselage uses a super-ellipse cross section due to the shape's high aerodynamic efficiency.

7.6 Payload Handling

The RFP emphasizes ease of maneuverability for loading and unloading the payload. The goal of the *Ibis* design is seamless integration into shipboard operations. Therefore, ground equipment that is currently in use in shipboard environments was selected. A dolly with an adjustable height bed, like the one pictures in Figure 49, is readily available in a shipboard operating space. With a dolly able to easily lift the heaviest payloads up to the *Ibis'* fuselage height, the team then considered the benefits and drawbacks of forward/backward/side loading for the payload.

The use of front loading through a door in the nose was ruled out since adding hinges and an opening would prohibit the placement of longerons and other support structures. The addition of a 50 kg (110.2 lb) payload would also have a drastic effect on the location of the CG. Loading through a door in the back of the fuselage was similarly ruled out due to the short stature of *Ibis* and the location of the tail boom, which does not leave enough room for a functional door to exist there. Side loading was deemed the simplest and most effective option. A basic hinge door that allows easy access to both the payload bay and the fuel tanks for refueling is placed on the port side of the aircraft fuselage.

Fig 49: Dolly

The height of the aircraft acts as a major limiting factor in the unloading process, forcing both the sailors and the disaster victims to crouch to open and close the payload door. A physical therapist was consulted to determine the best method for handling heavy payloads when some mechanical advantage is lost due to crouching. The results of this discussion are the inclusion of a handle on the outside of the payload box and the installation of a modular ramp. The handle

and ramp allow the ground team at the target location to easily and securely pull the payload out of the *Ibis* and out of reach of the rotor blades. This ramp is detailed further in Section 7.6.

Fig 50: Payload Door with Instructions

Fig 51: Retrieving Payload during Supplies Delivery Mission

Figures 50 and 51 show the payload door and ramp both open and in use. The door itself shows warning images and detailed directions on how to remove the payload and secure the door for *Ibis* to takeoff and return to the ship.

7.7 Internal Layout

The internal layout of the system was designed to be user-friendly and prevent unnecessary weight and wasted space. It was crucial that the weight distribution of the internal components does not degrade hover stability. Some

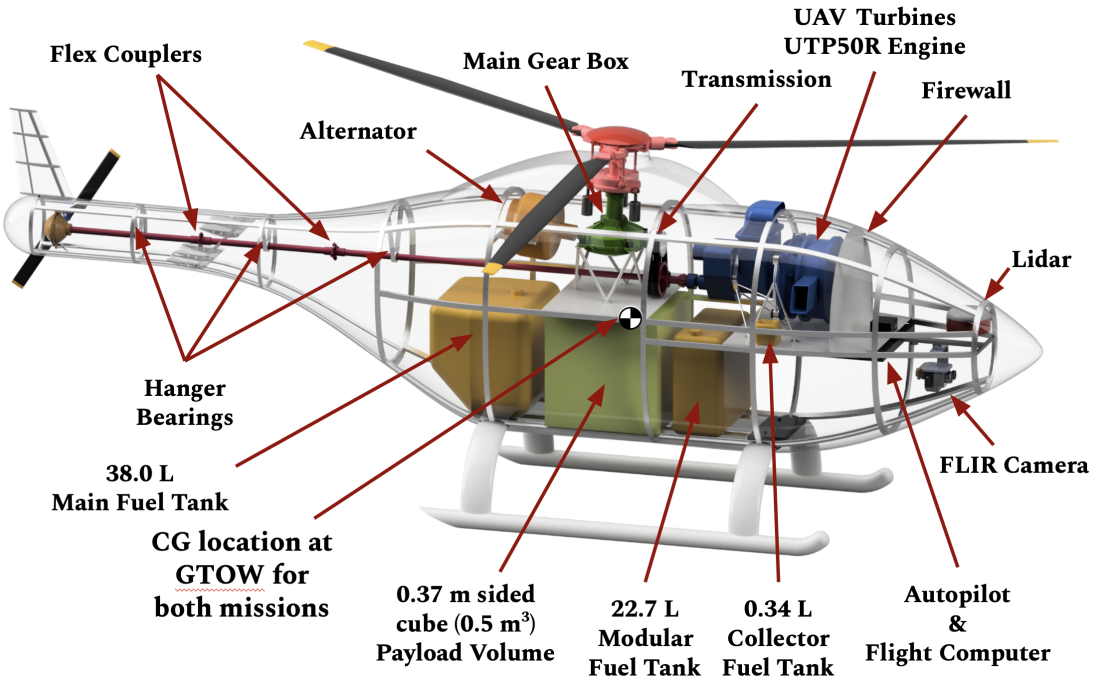

Fig 52: Internal Layout

key features of the internal layout include the transmission deck/engine deck, bolted to the bulkheads, that provides structural support for the engine and gearbox. Keel beams are located at the bottom of the fuselage and above the landing gear to reduce fuselage twisting and flexing. Multiple bulkheads are placed throughout the fuselage to insure the structural integrity from the semi-bulkhead located above the gearbox to the tail bulkheads along the empennage (Figure 52).

8 Vehicle Modularity

As referenced in the RFP, a system of modular add-ons can be used to help the vehicle meet the specific requirements set forth for each mission. When considering what type of modules to include, a conservative approach was taken in estimating how much can be accomplished in ten minutes on the deck of a ship. Simple actions like loading and unloading, securing doors and latches, and sealing tanks safely were all deemed reasonable. More ambitious modules, like adding complex avionics or different internal systems that would require more than five attachment points, were considered too complex to be swapped out in a safe and reliable manner, especially when the ship deck itself may be moving in a heavy sea state. In addition, the small size of the vehicle itself does not lend much elbow room for helping hands, thus reducing the amount of work that can reasonably be accomplished in ten minutes.

Ibis is able to complete both missions with the only one configuration. Therefore, all modularity is simply added to improve the efficiency and performance of the aircraft beyond the RFP requirements. Two areas were identified to more closely tailor *Ibis'* performance to each specific mission.

8.1 Payload Ramp

Ibis is tasked with delivering a supplies payload of 50 kg (110.2 lbs) over 185 km away from its takeoff point. Due to the height of the aircraft, 1.19 m (3.89 ft), removing this heavy payload poses a difficult task for an adult of average height trying to maneuver under stress. The first modular add-on is a removable ramp to help simplify this removal process of the supplies payload.

The ramp is conveniently stored next to the payload box (Figure 53) and is able to be removed, attached to a support beam with hooks, and used to pull the payload out and down onto the ground and out of reach from the rotor (. This helps keep the ground team safe by forcing them to stay low as they pull the payload out of the side of the vehicle rather than try and lift up. The handle on the payload box, as mentioned in section 7.6, gives the ground team member a better advantage than trying to grip only on the sides of the box in a tight space.

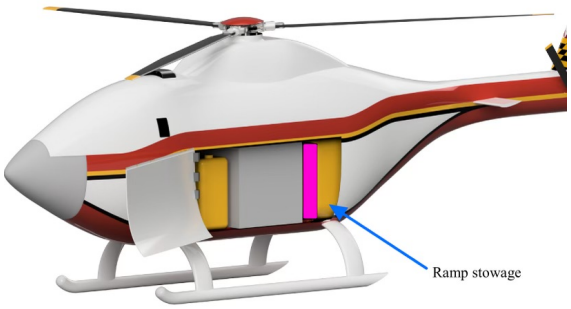

Fig 53: Ramp Stowage Location

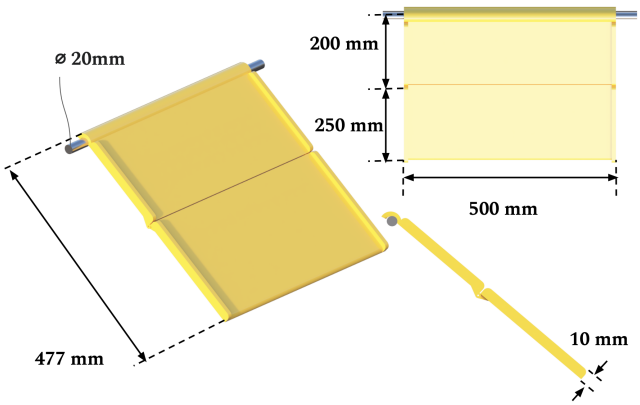

Fig 54: Ramp Dimensions

The ramp weighs 5 kg (11 lbs) and is made out of aluminum alloy, making it strong, yet light enough that even a child could remove, attach, and use it. Figure 55 details the concept of operations (ConOps) for each step of the process.

If *Ibis* is not flying a supplies delivery mission, the ramp can be easily removed on the ship deck under ten minutes by simply pulling it out of its pocket and transporting it back to the storage hangar to remove it as unnecessary weight. This can be done concurrently with loading the long endurance payload, since it can easily be placed on the dolly on which the endurance payload is being transported.

8.2 Removable Fuel Tank

The second opportunity identified to tailor *Ibis* for specific missions was to make one of the fuel tanks removable to conserve weight and create more space internally for a potentially larger payload. While the long endurance mission requires almost 47 kg of fuel, the supplies delivery mission requires merely one third of that.

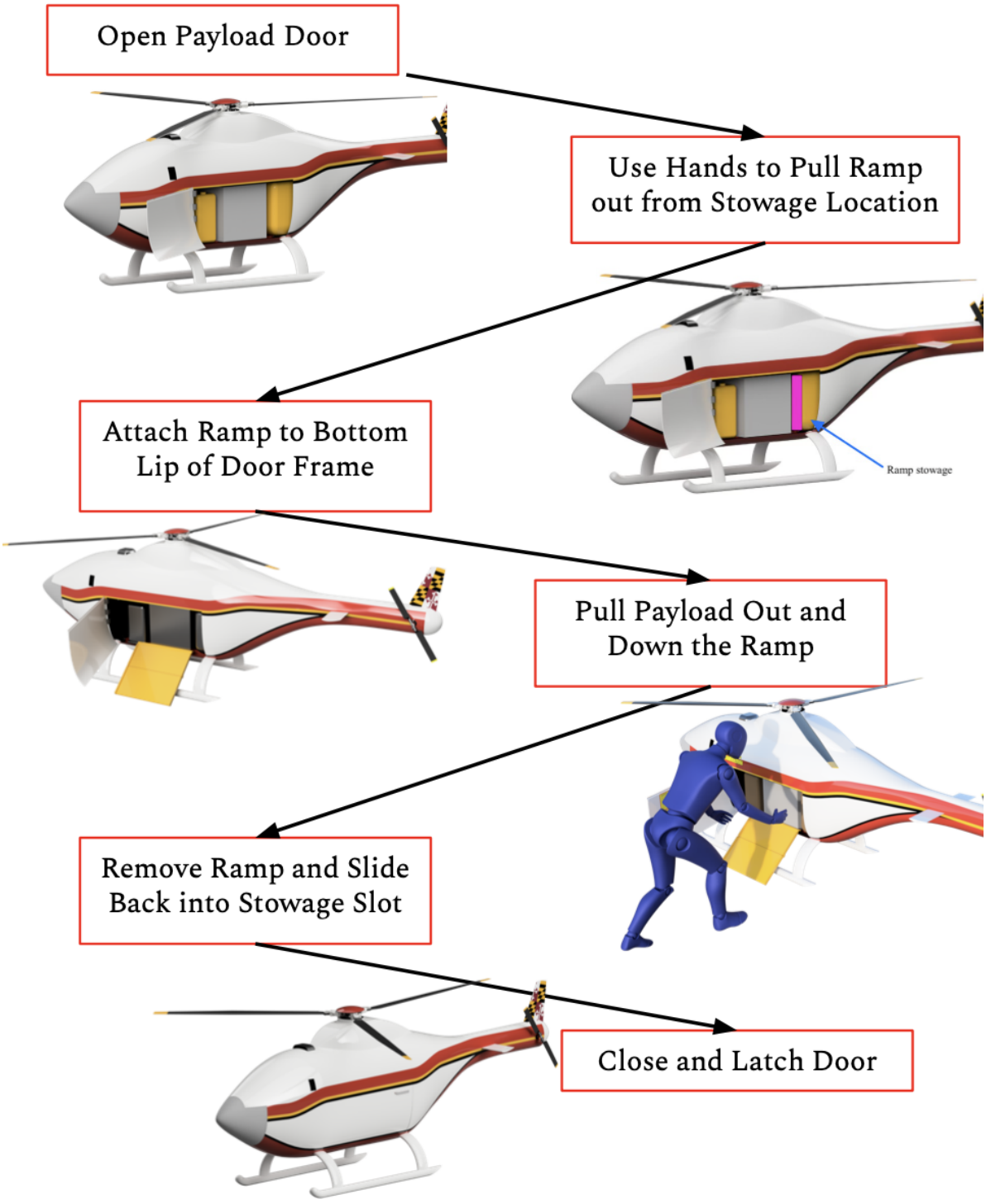

Fig 55: Con Ops for Ramp Module

The modular tank is the 22.7 liter (6 gal) tank that is located at the fore of the payload. The empty tank, made of Kevlar, weighs about 0.2 kg (0.45 lbs). The fuel tank is secured to the keel beams with four corner braces as well as strapped in with two ratchet straps over the top of the tank as shown in Figure 57. This attachment keep the fuel tank securely in place while also making it quick and easy to remove. The fuel pump is removed with the tank and the fuel line remains in the aircraft after being sealed with a rubber plug and secured to a bulkhead so it does not interfere

with any other parts of the aircraft. The ConOps for the fuel tank module removal process is shown in Figure 56. The installation process follows the same steps in the reverse order.

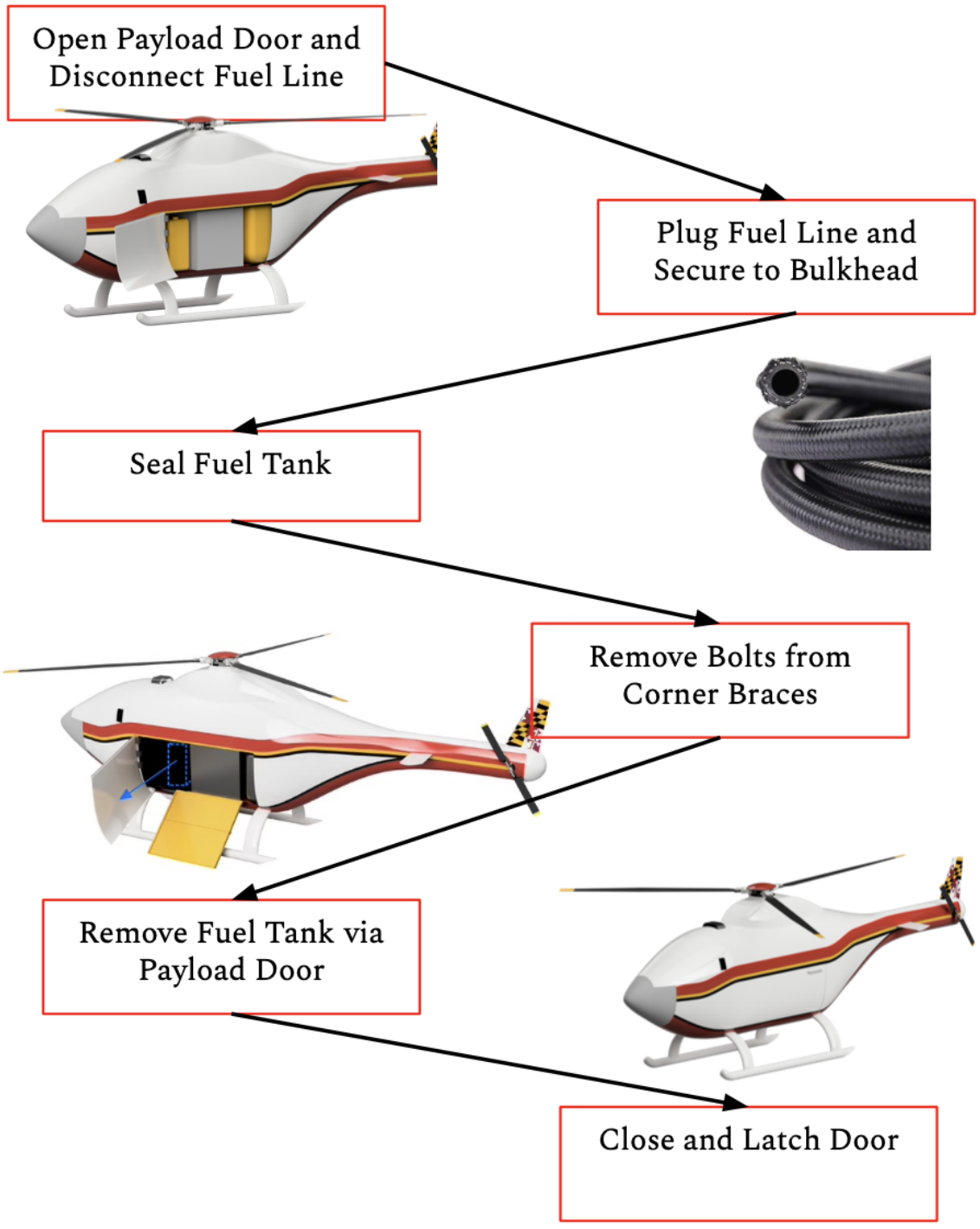

Fig 56: Con Ops for Fuel Tank Module

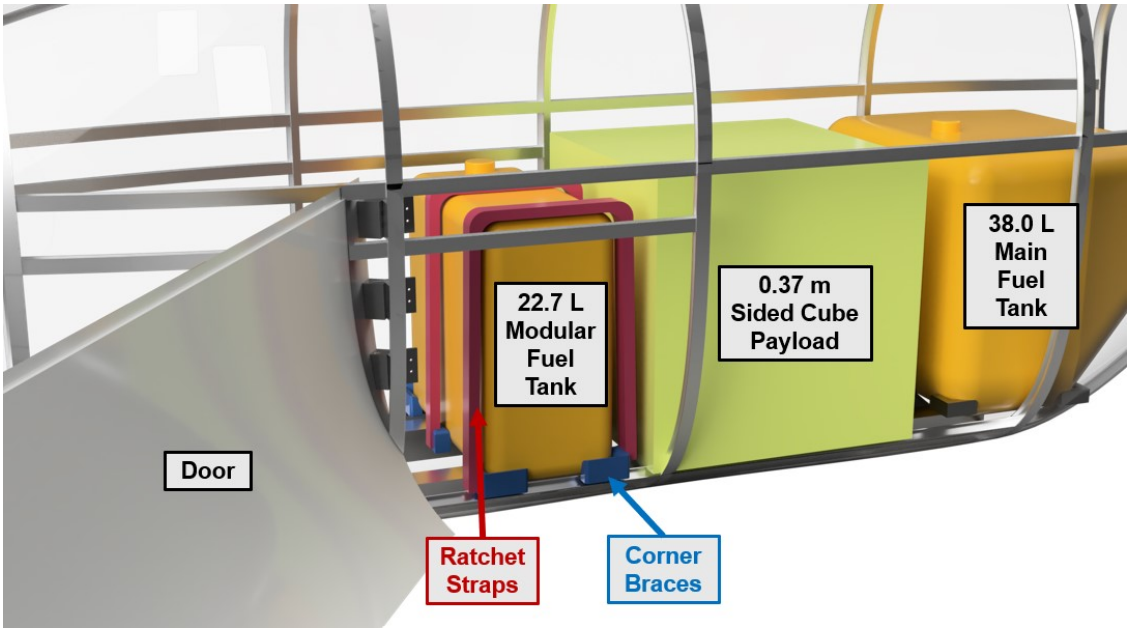

Fig 57: Modular Fuel Tank Mounting System

9 Avionics and Mission Equipment Package

9.1 Mission Overview

The avionics of *Ibis* are selected to be lightweight without sacrificing capability. Furthermore, *Ibis* uses currently available off-the-shelf technology. The wide variety of missions associated with disaster relief require the aircraft to be easily equipped with different sensor packages. *Ibis* offers extra computational capability to run mission specific software. Limitations in latency and bandwidth for Beyond Line of Sight (BLOS) communications necessitate that *Ibis* is capable of fully autonomous landing and navigation. While *Ibis* is able to conduct its mission without an operator, satellite communication (SATCOM) (Figure 58) enables an operator to intervene in case of unexpected circumstances or to re-task the vehicle.

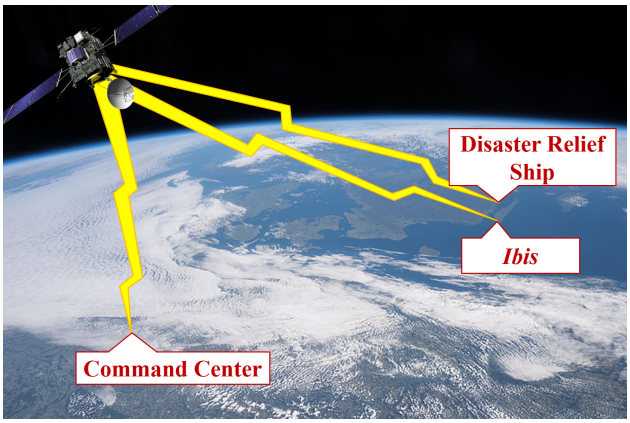

Fig 58: Communications System

- **Startup and Takeoff and Climb:** When *Ibis* is first powered on, the mission computer will run through a number of startup procedures to ensure that all of its sensors are functioning properly and there are no unexpected objects on the ship deck preventing takeoff. Using the integrated loudspeakers, *Ibis* will announce to bystanders that they need to stand back in multiple configurable languages. *Ibis* will then begin to spin up the blades. Once

the blades are at operating speed, the aircraft will wait in flight idle until it receives a signal from the command center to take off. The aircraft will then take off vertically and momentarily hover over the ship at an altitude of 10 m (33 ft). During this phase, the aircraft will use the 360-degree LiDAR to ensure that it does not hit the ship's superstructure. When the ship crew deems that the aircraft is ready to begin its mission, the aircraft will begin its ascent heading away from the superstructure until it is at an altitude of 50 m (164 ft) then turn towards its preassigned flight path as it finishes its climb to 500 m (1640 ft).

- **Forward Flight:** During forward flight, the aircraft will follow a predetermined flight plan while constantly scanning the horizon using the collision avoidance LiDAR and simultaneous localization and mapping (SLAM) to build a map of the terrain and other obstructions that it encounters. If obstructions are encountered, *Ibis* uses RRT* to find the new optimal path through the updated map. If *Ibis* determines that any path to the destination will require too much fuel, the aircraft will attempt to divert to the ship if possible, or to the nearest airport or landing area if not. Figure 59 shows a diagram of how *Ibis* processes data drawn in from it's sensors.
  - **Terrain Following Capability:** By incorporating radar altimeter measurements and LiDAR, *Ibis* can be instructed to follow contours in topography staying at a fixed altitude above the ground. This feature allows the aircraft to fly at low altitudes over mountainous terrain and is especially useful mapping disaster areas.

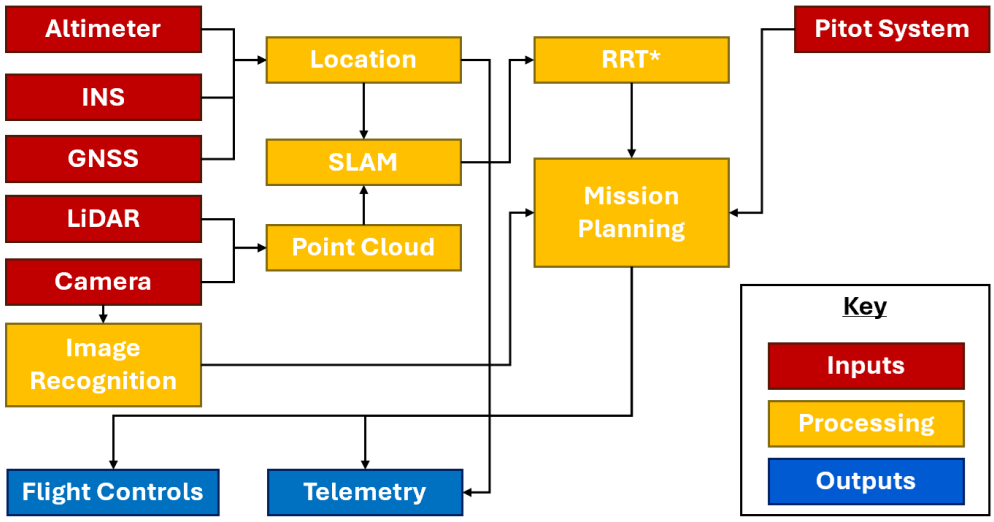

Fig 59: Mission Control Planning

- **Landing:** Once the aircraft is within 1 km (0.62 miles) of the landing zone's coordinates, *Ibis* begins searching for the helipad using the gimballed camera paired with optical object recognition. As *Ibis* approaches the landing pad, it fuses together images from three cameras located on the bottom of the aircraft into a 3D model using the SLAM algorithm. When landing, *Ibis's* sensors and cameras are able to seek, locate, and land within 1 m (3.3 ft) of the center of the landing zone. If the aircraft detects any unexpected obstructions, or bystanders on the helipad in the final stages of landing, it holds in a hover near the helipad and waits for the bystanders to leave the helipad. While landing, *Ibis* warns bystanders to stand back while the blades are still spinning. After the blades have stopped spinning verbal directions are given on how to safely unload the vehicle.

9.2 Sensors and Equipment

- **Autopilot:** *Ibis* is able to find its precise location using the VECTOR-600, see Figure 61(a), which integrates inertial navigations systems (INS) with global navigation satellite systems (GNSS). In the event that the aircraft is flying in a GPS-denied environment, the VECTOR-600 incorporates redundant INS giving *Ibis* a drift rate of less than 1.2km/hr (0.75mph), allowing the aircraft enough time to return to the ship or find a safe landing zone[20].

- **Forward Looking Infrared (FLIR)/Optical Camera:** To aid in search and rescue and general situational awareness, *Ibis* is equipped with a gimballed optical and long wavelength infrared (LWIR) camera. The FLIR Duo Pro R 640, displayed in Figure 61(b), allows *Ibis* to detect survivors' IR radiation, while also allowing the aircraft to look in any direction through a 4k optical camera[21].
- **360° LiDAR Puck:** *Ibis* comes equipped with an Innoviz360 LiDAR (Light Detection and Ranging) puck, Figure 61(c), capable of 360x64 Field of View (FOV) at 300 m (984 ft). This sensor was chosen as it is lightweight and capable of providing an exceptional FOV and resolution. The sensor is used to sense and deconflict with other air traffic and ground obstacles[22].
- **Mission Planning Computer:** Because of the heavy image processing requirements, *Ibis* comes equipped with high-end laptop components, shown in Figure 61(d), providing the perfect balance of high performance, weight, and power efficiency. *Ibis* mission control computer is a stripped-down ROG Scar 16 packing a NVIDEA RTX4090 and Intel i9-13980HX[23].
- **200MP Fixed Camera** *Ibis* stitches together video from three fixed cameras located on the bottom of the aircraft, see Figure 61(e).

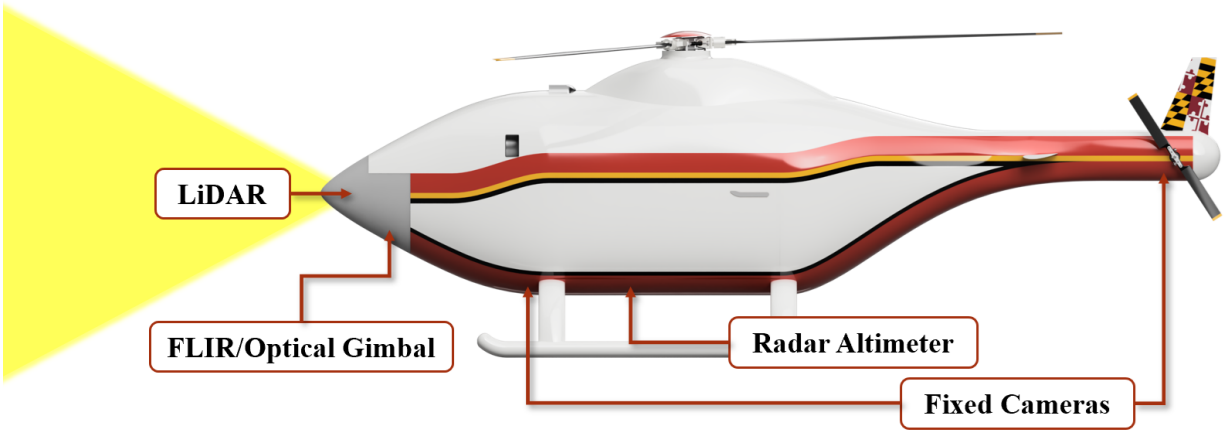

Fig 60: Location of Avionics Sensors

(a) **VECTOR-600 Autopilot Computer** (b) **FLIR Duo Pro IR/Optical Camera** (c) **INNOVIZ360 360° LiDAR puck** (d) **ASUS ROG Strix 16 Carrying a RTX4090 and i9-13980HX** (e) **High Resolution Cellphone Camera**

Fig 61: Main Avionics Components

9.3 *Safety*

Ibis can operate over urban regions and through congested airspaces. Furthermore, *Ibis* is expected to be handled by operators who may have little or no training on the platform. For these reasons safety was a major factor when designing *Ibis'* Avionics.

- **Lighting:** The FAA requires that helicopters have red and green anti-collision lights on the left and right respectively, a red strobe on the bottom nose and upper tail, and white strobe lights for landing.[24]
- **Aural Warnings:** To ensure safe usage by unskilled ground handlers, *Ibis* incorporates repeated verbal warnings before and while the blades are spinning. The language these warning are given in can be set ahead of time by the operator.
- **Emergency Protocols:** *Ibis* is capable of reacting to system failures minimizing the risk of financial loss or injury. During normal operation, *Ibis* is always searching for an emergency landing zone. In addition to relaying the aircraft's exact position to the ship via SATCOM, the aircraft relays the location of where it determines the best emergency landing zone is. This way, if the aircraft loses connection with the ship and must make an emergency landing it is easy to find and recover. Figure 62 shows *Ibis'* reaction to six of the most severe system failures.

Engine Failure

- To conserve energy in the battery, the aircraft will send off an SOS signal, and then enter low-power mode.
- The aircraft will attempt an auto rotation down to a predetermined emergency landing zone (PELZ)

Loss of Communication

- In the event of loss of communication, the aircraft will continue to carry out its mission unless the aircraft is in easy-recovery mode.
- In easy-recovery mode, the aircraft will land at the PELZ

Alternator/Battery Failure

- In the event of an alternator or battery failure, the aircraft will switch to the alternate electrical source and enter low power mode.
- The aircraft will then land at the PELZ

Mission Control Computer Failure

- The mission control computer runs three separate instances of the flight control software through separate VMs (virtual machines).
- If one of the instance crashes, outputs a bad commands, the aircraft can safely reboot that VM

Bad LiDAR returns

- If the Ibis detects that the LiDAR is not functioning properly, the aircraft will immediately land at the PELZ.
- The aircraft cannot fly safely if it is unable to detect obstacles or air traffic.

Fixed Camera Failure

- In the case that one of the fixed cameras fails, or is obstructed, the helicopter will continue along its flight plan and attempt to land normally, as the aircraft only needs two cameras to land.

Fig 62: *Ibis'* Emergency Protocols

9.4 *Weight Breakdown of Avionics Equipment*

The avionics of *Ibis* were designed to be as lightweight and power efficient as possible without sacrificing capability. Table 15, shows the total weight and power consumption of the avionics components. The table also show the severity of failure for the component according to MIL-STD-882.

- Cat I: Loss of the component could cause death or damage costing $10M
- Cat II: Loss could cause permanent injury or damage totaling between $1M-$10M
- Cat III: Loss could cause reversible injury or damage totaling between $100K-$1M
- Cat IV: Could reverse in minor injury, or damage totaling less than $100K

Ibis' avionics offer a comprehensive solution that ensures full autonomy, safety, and simplicity. By integrating currently available hardware, it allows the aircraft to operate independently with minimal human intervention. The system's design prioritizes ease of use, making it accessible and straightforward for operators. Moreover, *Ibis'* avionics are constructed using components that are readily available on the market today, reducing the cost of maintenance.

Name	Quantity	Mass (kg)	Mass (lbs)	Net Power (W)	Cost ($)	Severity of Failure MIL-STD-882
Autopilot	1	0.18	0.397	2.5	15000	Cat I
Radio Amplifier	1	0.3	0.661	25	1000	Cat III
SatComm	1	0.3	0.661	25	500	Cat IV
Power Management System	1	0.3	0.661	5	500	Cat II
Flight Control Computer	1	1.36	2.998	330	3700	Cat I
FLIR/Optical Camera	1	0.325	0.717	10	600	Cat IV
Camera Gimble	1	0.36	0.794	9.6	300	Cat IV
LIDAR	1	1	2.205	25	25000	Cat III
Transceivers' comm antennas	3	0.6	1.323	3	500	Cat III
GPS Antennas	1	0.1	0.22	1	1000	Cat III
Radar Altimeter	1	0.3	0.661	11	5000	Cat III
Pitot System	1	1	2.205	102	500	Cat IV
Fixed Cameras	3	0.03	0.066	1.8	600	Cat I
Loud Speaker	1	0.5	1.102	15	500	Cat IV
Total		**6.655**	**14.67**	**565.9**	**54700**	

Table 15: Weight Breakdown of Avionics Equipment

10 Vehicle Performance

10.1 Parasite Drag Estimation

Parasite drag estimation was made using methods outlined by Prouty [25]. Fuselage drag was estimated as a combination of skin friction and pressure. Frontal and planform areas for each component (rotor hubs, landing gear, and empennage) were measured from vehicle drawings and combined with empirical factors from Prouty [25] to calculate individual component equivalent flat plate areas. These values were summed to determine the equivalent flat plate area of the entire helicopter (Table 16). An additional 20% was added to the total for more realistic results as recommended by Prouty. This refined analysis resulted in an estimated total equivalent flat plate area of 0.117 m^2 (1.26 ft^2). The fuselage contributed the highest percentage of total drag, followed by the main rotor hub and landing gear. The landing gear, despite being a fixed skid landing gear, only contributes 10.87% of total drag due to the aerodynamic elliptical cross section of the cross tubes.

Table 16: Equivalent Flat Plate Area Drag Breakdown

Component	Eq. Flat Plate Area - m^2 (ft^2)	Percent of Total
Fuselage	0.038 (0.406)	38.59
Landing Gear	0.011 (0.114)	10.87
Main Rotor Hub	0.031 (0.333)	31.63
Tail Rotor Hub	0.005 (0.054)	5.12
Empennage (Vertical and Horizontal Tails)	0.001 (0.009)	0.84
Roughness and Leakage	0.004 (0.041)	3.86
Protuberances (Antennas, Vents, Drains)	0.008 (0.091)	8.62
Engine Cooling	0.0005 (0.005)	0.48
Total	**0.098 (1.052)**	**100.00**
+20%	**0.117 (1.263)**	-

Flat plate areas were used to estimate the component by component drag forces during the long-endurance mission segment 5 and supplies-delivery mission segment 4. The dynamic pressure and skin friction coefficient (used in fuselage drag estimation) varies between these two mission segments. Dimensional drag forces are shown in Table 17.

CFD analysis through SolidWork's Flow Simulation software was used to predict the lift area and pitching moment volume of the vehicle airframe in trimmed flight with zero pitching and yawing angle. The results for the main rotor hub and fuselage are shown in Figures 63, 64. High pressure regions are indicated in red, and low pressure regions are indicated in dark blue. The fuselage contractions are smooth to ensure no flow separation along the fuselage. The

Table 17: Drag Force Breakdown

Component	Long-Endurance Segment 5 - N (lb)	Supplies-Delivery Segment 4 - N (lb)
Fuselage	23.97 (5.39)	73.88 (16.61)
Landing Gear	6.43 (1.45)	20.69 (4.65)
Main Rotor Hub	18.71 (4.21)	60.20 (13.53)
Tail Rotor Hub	3.03 (0.68)	9.75 (2.19)
Empennage (Vertical and Horizontal Tails)	0.49 (0.11)	1.59 (0.36)
Roughness and Leakage	2.51 (0.56)	7.38 (1.66)
Protuberances (Antennas, Vents, Drains)	5.21 (1.17)	16.46 (3.70)
Total	**60.35 (13.63)**	**189.96 (49.91)**

lift area is 0.0054 m^2 (0.0583 ft^2) and the pitching moment volume is 0.0122 m^3 (0.4304 ft^3). The calculated drag area from CFD is 0.0446 m^2 (0.48 ft^2). However, the more conservative estimate of 0.088 m^2 (0.951 ft^2) based upon empirical estimates outlined by Prouty (Table 16) was used in performance analysis.

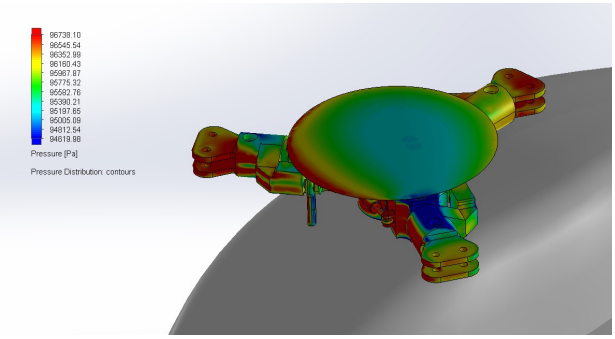

Fig 63: CFD of Main Rotor Hub in Cruise

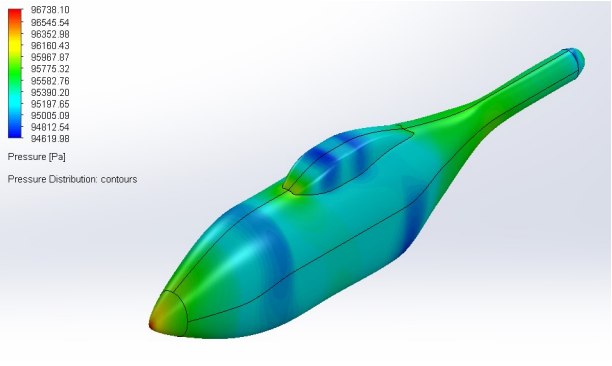

Fig 64: CFD of Fuselage in Cruise

10.2 Forward Flight Performance

The airspeed that *Ibis* operates at is a function of the mission segment requirements and aircraft weight. Because the aircraft weight decreases by $\sim 40\%$ during both mission, *Ibis* operates at different speeds throughout a flight. For loitering, the best airspeed is the airspeed corresponding to minimum power consumption - velocity of best endurance (VBE). However, for cruise segments, the best airspeed is one that burns the least fuel for a given distance. Turboshaft engines operating at suboptimal conditions operate less efficiently with a higher specific fuel consumption (SFC). An empirical model of various production gas turbine engines [26] models this effect using equation 4.

$$SFC = SFC_{\text{base}} \left(\frac{P_{\text{required}}}{P_{\text{installed}}} \right)^{-0.256} \tag{4}$$

Using this model, the velocity for highest specific range (greatest distance/mass of fuel) is found to be higher than the velocity for best range (VBR) when considering vehicle power alone. *Ibis* flies at the velocity of highest specific range during the cruise segments of both missions - to and from the destination. Note, that this velocity changes between the inbound and outbound cruise segments.

Ibis can complete the long endurance mission at a GTOW of 156.74 kg (345.56 lbs). Figure 65 shows the power required to cruise and loiter at various speeds. The loiter speed for segment 5 in the endurance mission is 28.7 m/s (55.9 kts) to minimize power usage and thus fuel consumption. Figure 66 shows the specific range during cruise and loiter at various speeds. The cruise speed to the destination (segment 4) is 51.4 m/s (100.0 kts) while the return flight (segment 6) is completed at a slightly lower speed of 48.8 m/s (94.8 kts). The minimum flight speed for segment 4 is 41.1 m/s (78.3 kts) to travel 185 km in 75 minutes, so *Ibis* operates at the best speed for limiting fuel consumption.

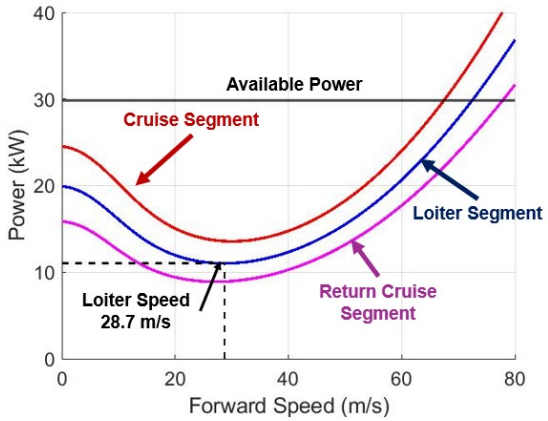

Fig 65: Long Endurance Mission Level Flight Performance in Cruising and Loitering Mission Segments at the Minimum Required GTOW

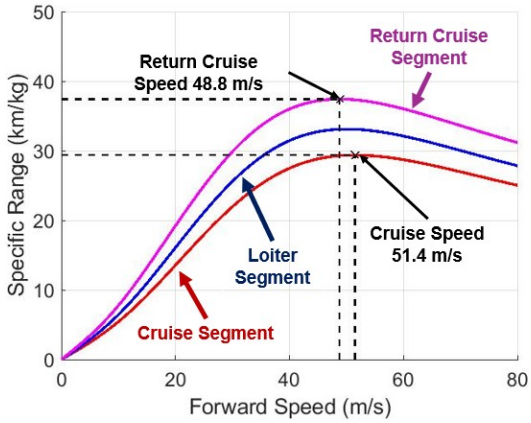

Fig 66: Long Endurance Mission Specific Range in Cruising and Loitering Mission Segments at the Minimum Required GTOW

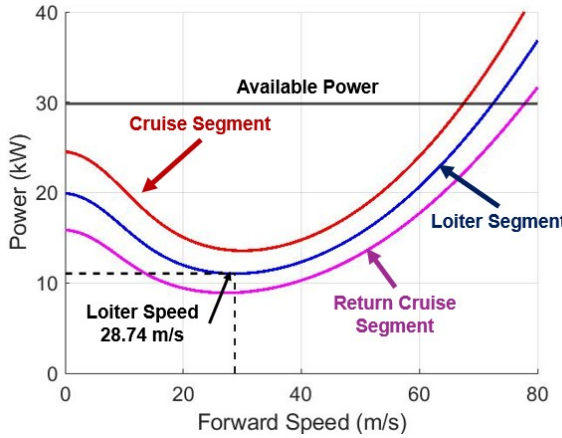

Fig 67: Long Endurance Mission Level Flight Performance in Cruising and Loitering Mission Segments at the Maximum Available GTOW

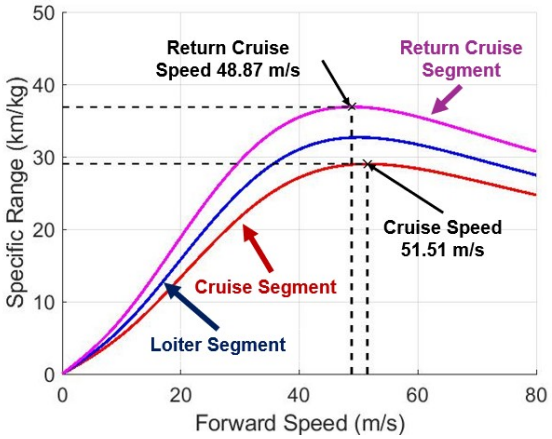

Fig 68: Long Endurance Mission Specific Range in Cruising and Loitering Mission Segments at the Maximum Available GTOW

However, *Ibis* must also be capable of completing the long endurance mission at a GTOW of 160 kg (352.7 lbs), therefore the forward flight performance is evaluated at this greater weight. For the heavier GTOW, the cruise speed increases to 51.5 m/s (100.1 kts) in segment 4 and 48.9 m/s (95.0 kts) in the return flight (segment 5) as shown in Figure 68. The endurance mission loiter speed also increases to 28.74 km/h (55.9 kts) as shown in Figure 67. These speeds are less than 1% increase from the minimum GTOW operating speeds, and as such, operating at the lower speed negligibly effects the overall performance of the vehicle. For operational simplicity, the vehicle flies at the lower speeds of 51.4, 28.7, 48.8 m/s in segments 4, 5, and 6 respectively.

The supplies delivery mission can be completed with a GTOW of 149.87 kg (330.41 lbs). The mission contains a short loiter spanning 20 minutes before the vehicle must descend and unload its payload. The best loitering speed is 29.74 m/s (58.0 kts) as shown in Figure 69. Shown in Figure 70, the cruise speed in segment 4 is 51.35 m/s (99.8 kts), the same as the endurance mission, and the returning cruise speed is 48.0 m/s (93.3 kts). Maximizing the GTOW to 160 kg marginally increases the forward flight speeds. Similarly to the long endurance mission, *Ibis* operates at the speeds defined by the minimum required GTOW for operational simplicity.

The loitering endurance of *Ibis* in the long endurance mission is shown in Figure 71. Note that an increase in payload directly displaces fuel weight because the GTOW is fixed at 160 kg for all missions. The long endurance mission can be accomplished with a vehicle GTOW below 160 kg (352.7 lbs). The mission can be expanded to either

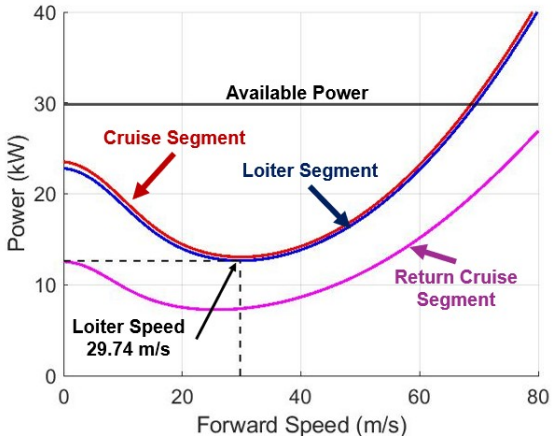

Fig 69: Supplies Delivery Mission Level Flight Performance in Cruising and Loitering Mission Segments at the Minimum Required GTOW

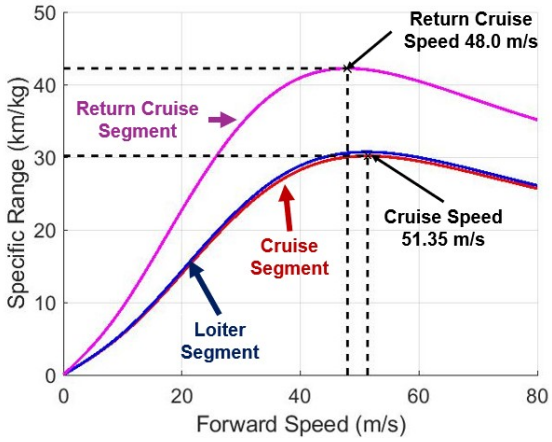

Fig 70: Supplies Delivery Mission Specific Range in Cruising and Loitering Mission Segments at the Minimum Required GTOW

carry a larger communications payload of 22.2 kg (48.94 lbs) for ten hours of loiter or carry the existing 20 kg payload for 10.8 hours of loiter. Both missions require an additional modular fuel tank. By exchanging the payload for fuel, the maximum possible endurance is 18.1 hours.

The delivery range of *Ibis* is shown in Figure 72. The required distance for supplies delivery is 185 km (115 miles), and *Ibis* can accomplish this mission with a vehicle GTOW below 160 kg (352.7 lbs). The mission can be expanded for a greater distance of 342 km (212.5 miles) or a larger supply package of 59.3 kg (130.7 lbs) as shown in Figure 72. By exchanging the payload for fuel, a maximum range of nearly 1200 km (745 miles) is possible.

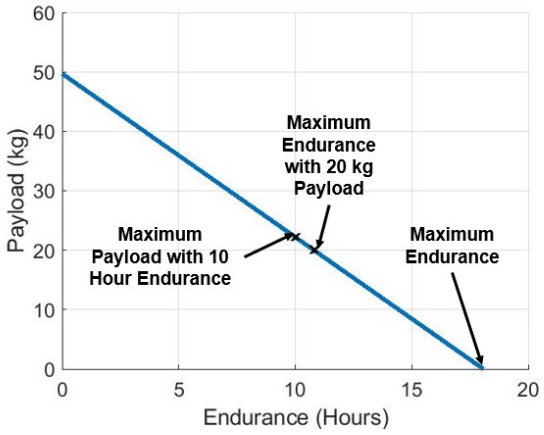

Fig 71: Loitering Endurance in Long Endurance Mission with a Specified Payload

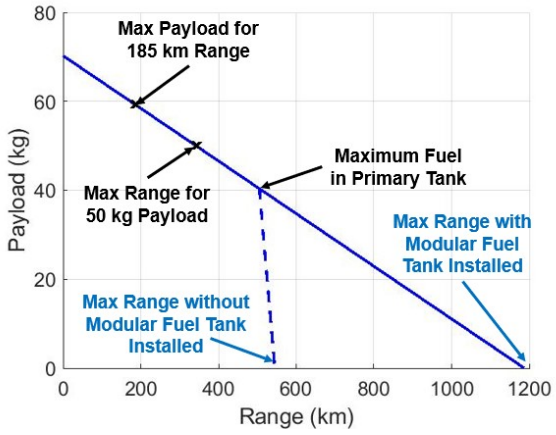

Fig 72: Range of Vehicle for Supplies Delivery with a Specified Payload

10.3 Hover and Climb Performance

The hover performance of *Ibis* at a GTOW of 160 kg as altitude increases is shown in Figure 73. A transmission of 29.4 kW has been imposed on the design to reduce the weight of the transmission. The maximum altitude the vehicle can maintain hover is 3145 m (10300 ft) which exceeds the mission cruise and loiter altitude of 500 m (1640 ft). The axial and cruising rate of climb (ROC) as altitude increases is shown in Figure 74. The axial climb is limited by the available power from the engine and further limited by the transmission with a maximum hovering service ceiling of 3040 m (9970 ft). The cruising climb at a cruise speed of 51.4 m/s (100.0 kts) (cruise speed during long endurance mission) can reach higher altitudes. The vehicle stalls at 6100 m (20000 ft) and cannot climb any further.

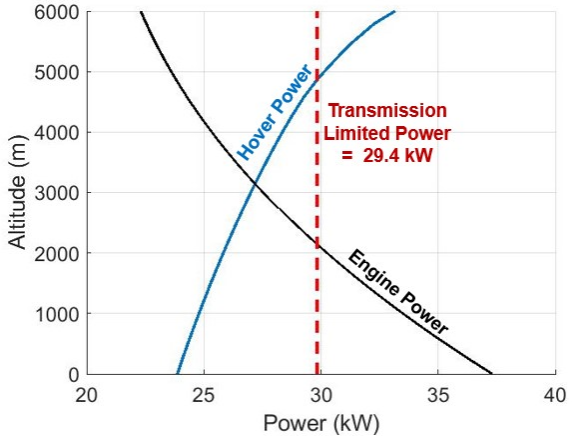

Fig 73: Hover Power Requirement at GTOW = 160 kg at Altitude

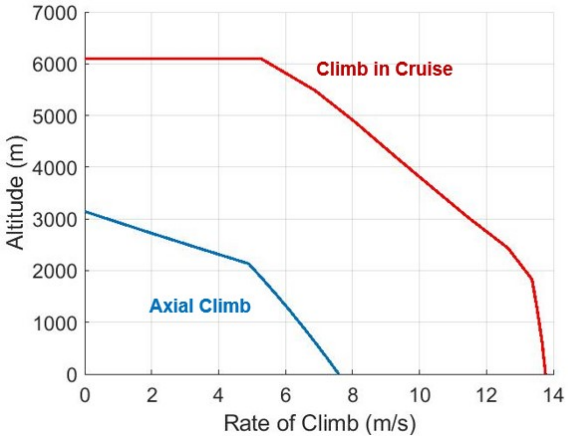

Fig 74: Axial and Cruising Rate of Climb at Altitude

The rate of climb (ROC) of *Ibis* at sea level shown in 75 corresponds to a GTOW of 160 kg and an empty weight of 87.87 kg (193.73 lbs). The maximum ROC is substantially higher than necessary to complete the climb segments of both missions which requires a minimum ROC of 2.08 m/s (409.8 ft/min) to climb 500 m in 4 minutes. To minimize power consumption, the vehicle is set to climb at 2.08 m/s.

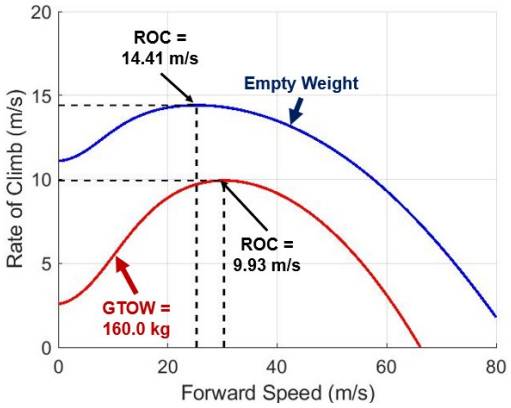

Fig 75: Climb Performance at Sea level

10.4 Mission Segment Performance and Weight

For each mission segment of both missions, the vehicle weight, total power requirement, aerodynamic power requirement, transmission efficiency, and powerplant efficiency are shown in Table 18 and Table 19 for the supplies delivery mission. Based on the thermal efficiency of an engine defined in Eqn. 5 as the ratio between lower calorific value (LCV) and specific fuel consumption (SFC), the powerplant efficiency (η) is calculated at each segment. The LCV of Jet-A fuel is 43.15 MJ/kg [27]. In compliance with mission requirements, the GTOW for both missions is 160 kg.

$$\eta = \frac{1}{SFC} * \frac{1}{LCV} \tag{5}$$

Table 18: Vehicle Performance in the Long Endurance Mission

Mission Segment	Starting Weight kg (lbs)	Total Power kW (HP)	Aerodynamic Power kW (HP)	Transmission Efficiency	Powerplant Efficiency
Segment 1	160.00 (352.73)	4.76 (6.39)	3.15 (4.22)	0.95	0.20
Segment 2	159.84 (352.37)	21.46 (28.78)	18.41 (24.68)	0.95	0.30
Segment 3	159.83 (352.36)	21.45 (28.77)	18.39 (24.67)	0.95	0.30
Segment 4	159.43 (351.47)	18.95 (25.42)	9.41 (12.61)	0.95	0.29
Segment 5	153.85 (339.18)	13.77 (18.46)	8.14 (10.92)	0.95	0.26
Segment 6	115.55 (254.75)	13.82 (18.53)	5.90 (7.91)	0.95	0.27
Segment 7	110.87 (244.42)	16.20 (21.73)	13.65 (18.30)	0.95	0.28
Segment 8	110.54 (243.70)	16.01 (21.47)	13.47 (18.06)	0.95	0.28

Table 19: Vehicle Performance in the Long Endurance Mission

Mission Segment	Starting Weight (kg, lbs)	Total Power (kW, HP)	Aerodynamic Power (kW, HP)	Transmission Efficiency	Powerplant Efficiency
Segment 1	160.00 (352.73)	4.76 (6.39)	3.15 (4.22)	0.95	0.20
Segment 2	159.88 (352.47)	21.14 (28.36)	18.12 (24.30)	0.95	0.30
Segment 3	159.87 (352.45)	21.14 (28.35)	18.11 (24.29)	0.95	0.30
Segment 4	159.44 (351.50)	18.95 (25.42)	9.41 (12.61)	0.95	0.29
Segment 5	154.20 (339.94)	13.83 (18.54)	9.88 (13.25)	0.95	0.27
Segment 6	152.75 (336.75)	20.26 (27.17)	17.32 (23.22)	0.95	0.29
Segment 7	152.37 (335.90)	20.24 (27.14)	17.30 (23.20)	0.95	0.29
Segment 8	102.36 (225.66)	15.27 (20.48)	12.82 (17.19)	0.95	0.27
Segment 9	102.35 (225.64)	11.27 (15.11)	9.20 (12.34)	0.95	0.25
Segment 10	102.10 (225.09)	12.60 (16.89)	5.10 (6.84)	0.95	0.26
Segment 11	97.93 (215.89)	14.79 (19.83)	12.37 (16.59)	0.95	0.27
Segment 12	97.63 (215.23)	14.62 (19.61)	12.27 (16.45)	0.95	0.27

11 Aircraft Acoustics

11.1 Broadband Noise

Ibis operates in the close vicinity of people, both at the ship deck and disaster area. Thus, low noise is a desirable quality. An estimate of the broadband noise of *Ibis'* rotor is made using a new empirical model developed by Gill and Lee [28]. A comprehensive data set of wide encompassing rotor noise tests and a genetic algorithm was used to develop this acoustics model.

The model follows the coordinate system in Figure 76, where the observer is located at an elevation θ_0 and distance s_0 from the rotor axis. The overall sound pressure level (OASPL) can be found using equations 11.1, where $\beta_1 = 0.01$, $\beta_2 = 9.25$, and $\beta_3 = 0.73$. D refers to the rotor diameter.

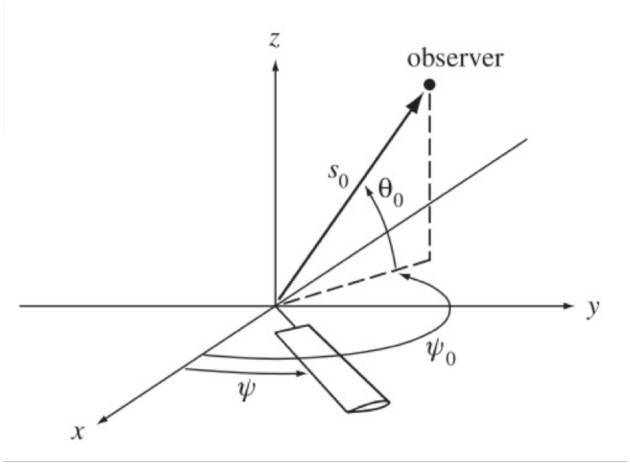

Fig 76: Model Coordinate System

$$\begin{aligned} \text{OASPL} &= \left(\sin^{\beta_1}|\theta_0|\right)\text{OASPL}_{\text{ref}} - \left(\beta_2 + \beta_3\left(1 - \sin|\theta_0|\right)\right)\log\left(\frac{s_0}{D}\right) \\ \text{OASPL}_{\text{ref}} &= 10\log_{10}\left(V_t^{6.77}\cdot C_T^2\cdot\sigma^{-1}\right) - 32.73 \end{aligned} \tag{6}$$

The broadband OASPL for an observer 150m below *Ibis* due to the rotor is 73.5 dB. This result is within the range of other existing drones and helicopters [28].

12 Vehicle Cost

Two models were used to estimate cost of the aircraft; Harris and Scully [29] and a method from Bell Helicopters [30]. The Harris and Scully model is based on an analysis of 72 helicopters and their cost breakdown. Based on 2008 dollars, the equation is shown in 7.

$$BasePrice = 345 * H * N_b^{0.2045} * W_0^{0.4854} * P^{0.5843} \tag{7}$$

Where:
H = Engine Type
N_b = Number of Main Rotor Blades
W_0 = Empty Weight (lb)
P = Engine Rated Power (HP)

Based on the materials, airframe, and engine the team looked at, our airframe purchase formula inputs were the following:
$H = 1.779$ (Gas Turbine Engine)
$N_b = 3$
$W_0 = 195.7$ lb
$P = 50$ HP

Thus: $BasePrice$ = \$97,860

After adjusting for inflation, the true base price is = \$143,000. The avionics make up the most costly addition to the base price. *Ibis'* avionics are estimated to cost \$55,000, bringing the true estimation for one *Ibis* aircraft to be \$198,000.

Fig 77: Yamaha R-Max

Fig 78: Schiebel Camcopter

The second method, the Bell Helicopter model, takes many more variables into account and is based on total production quantity and production rate in one year. The results from this method provide a comparison with the Harris and Scully estimate and are shown in Table 20.

Table 20: Bell Model Cost Breakdown

Aircraft Subsystem	**Cost ($)**
Main Rotor	8,860
Tail Rotor	1,170
Avionics	55,000
Airframe	50,700
Powerplant	37,000
Final Assembly	50,000
Total Cost:	**202,730**

For a production quantity of 1000 aircraft at a rate of 100 produced per year, the total cost of production for one *Ibis* aircraft is $202,730.

Both the Bell and Harris and Scully models corroborate an estimated cost of around $200,000 to produce an *Ibis* aircraft. A further corroboration was obtained by researching the cost of existing UAVs of similar size and capabilities to compare the prices. The Yamaha R-MAX, which has a GTOW of 94 kg, a 3.1 m rotor diameter, and 1 hour long endurance, is currently on the market for $100,000 (Figure 77) [31]. The Schiebel Camcopter S-100, with a GTOW of 110 kg, maximum payload of 50 kg, and an endurance of 6 hours, costs around $400,000 (Figure 78) [32]. Comparing the relative performance and price of the *Ibis* with both of these UAV competitors, *Ibis'* cost estimate is both reasonable and feasible.

In addition to completing the supplies delivery and long endurance missions set forth by the RFP, *Ibis* will not sit by idle waiting for disaster to strike. Due to its simple mechanics and low maintenance design, Ibis is truly a low cost solution to a multitude of problems. Alternate uses for the vehicle include commercial delivery, agricultural monitoring, and search and rescue.

13 Weight Analysis

13.1 Weight Breakdown

The empty weight of *Ibis* is 87.86 kg (193.73 lbs), which is defined with zero usable fuel and no onboard payload. The aircraft's total weight at engine start is 160 kg (352.8 lbs) for both missions. Lower weights can fulfill both missions with the removal of the additional fuel + payload for a total weight of 149.86 kg (330.38 lbs) for the supplies delivery mission and 156.73 kg (345.53 lbs) for the long endurance mission. The additional fuel and payload weight can be used to expand the mission for longer endurance or larger supply packages. Component weights are calculated from CAD software by assigning material properties to part geometry. The complete weight breakdown is shown in Table 21.

Table 21: Weight Breakdown

Component		Weight - kg (lb)	% of Empty Weight
Rotors	Main	6.93 (15.27)	7.88
	Tail	0.11 (0.24)	0.12
Airframe	Skin	8.73 (19.25)	9.94
	Frame	7.74 (17.08)	8.82
	Paint	0.38 (0.83)	0.43
	Door	2.78 (6.12)	3.16
	Horizontal Tail	0.16 (0.34)	0.18
	Vertical Tail	0.12 (0.26)	0.13
Landing Gear		5.59 (12.32)	6.36
Propulsion	Engine	34.85 (76.85)	39.67
	Alternator	4.04 (8.90)	4.59
	Firewall	0.19 (0.41)	0.21
Fuel System	Fuel Tank Main	0.29 (0.64)	0.33
	Modular Fuel Tank	0.18 (0.40)	0.21
	Collector	0.01 (0.02)	0.01
Drive System	Main Gear Box	6.69 (14.75)	7.61
	Tail Drive Shaft	1.77 (3.89)	2.01
	Tail Gear Box	0.47 (1.03)	0.53
Avionics		6.86 (15.12)	7.80
Empty Weight		**87.86 (193.73)**	100.00
Fuel Weight - Supplies		12.00 (26.45)	
Fuel Weight - Endurance		48.87 (107.74)	
Payload - Supplies		50.00 (110.25)	
Payload - Endurance		20.00 (44.10)	
*Additional Fuel + Payload - Supplies		10.14 (22.35)	
*Additional Fuel + Payload - Endurance		3.27 (7.21)	
GTOW		**160.00 (352.74)**	

* Additional Fuel + Payload is added usable load beyond the base mission profiles.

13.2 Center of Gravity Analysis

Ibis' center of gravity (CG) variation in all principle axes is shown in Figure 79, Figure 80, and Figure 81. The datum point for the CG position is situated longitudinally (x) along the main rotor axis, laterally (y) with the axis of symmetry, and vertically (z) in relation to tail rotor height. CG movement is positive aft longitudinally, upward vertically, and rightward laterally. The longitudinal CG remains in front of the main rotor axis in both missions and is 0.169 m (6.65 in) at the farthest with a vehicle weight equivalent to empty weight. At GTOW, the supplies delivery mission has a slightly closer CG position to the main rotor axis at 0.036 m (1.42 in). The lateral CG remains on the port side of the aircraft for both missions with its maximum at 0.0052 m (0.20 in) leftward of the axis of symmetry for the empty weight vehicle. The minimum distance is 0.0028 m (0.11 in) leftward at GTOW. The lateral CG shifts minimally throughout missions. The vertical CG remains below the tail rotor axis. The empty weight vehicle is closest at 0.038 m (1.5 in) below the tail rotor, whereas the farthest distance is 0.14 m (5.5 in) at GTOW.

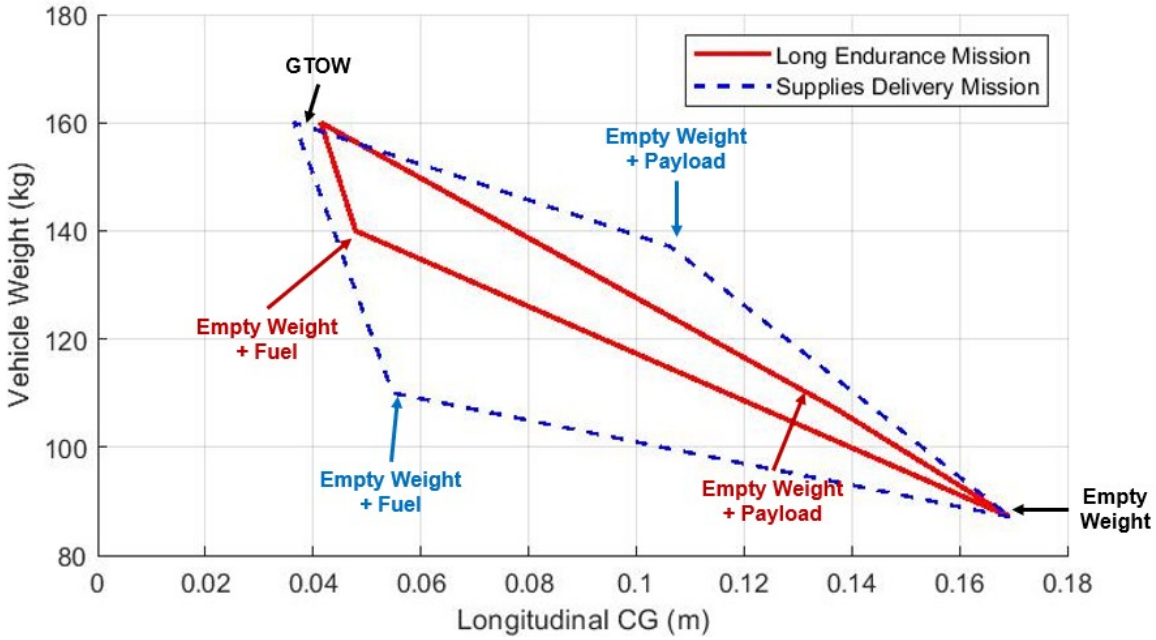

Fig 79: Vehicle Longitudinal CG Variation (Positive Aft)

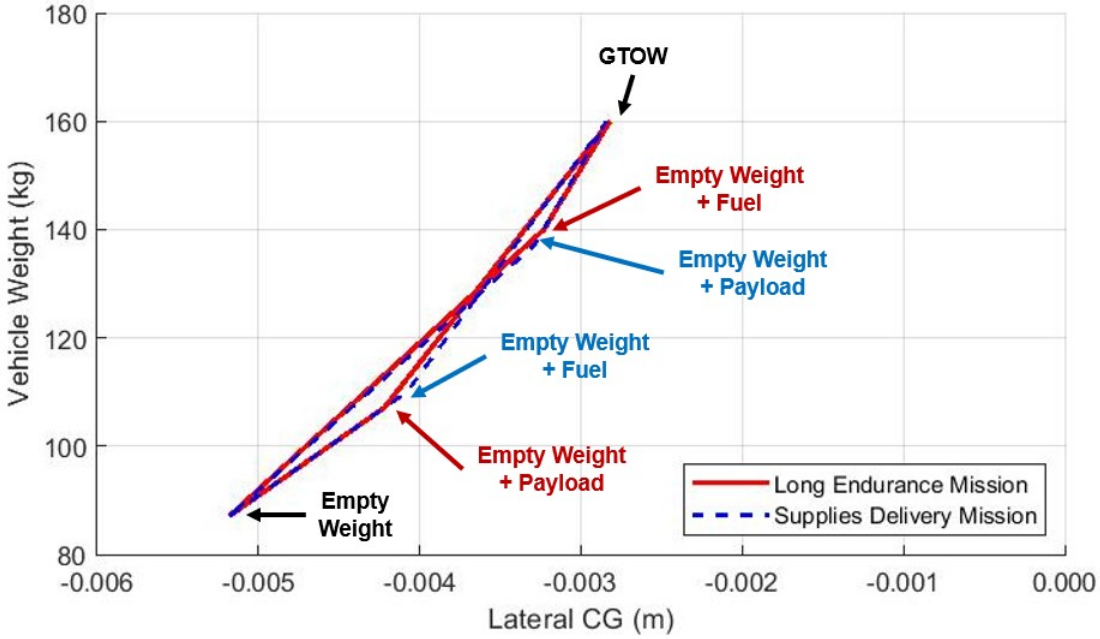

Fig 80: Vehicle Lateral CG Variation (Positive Starboard)

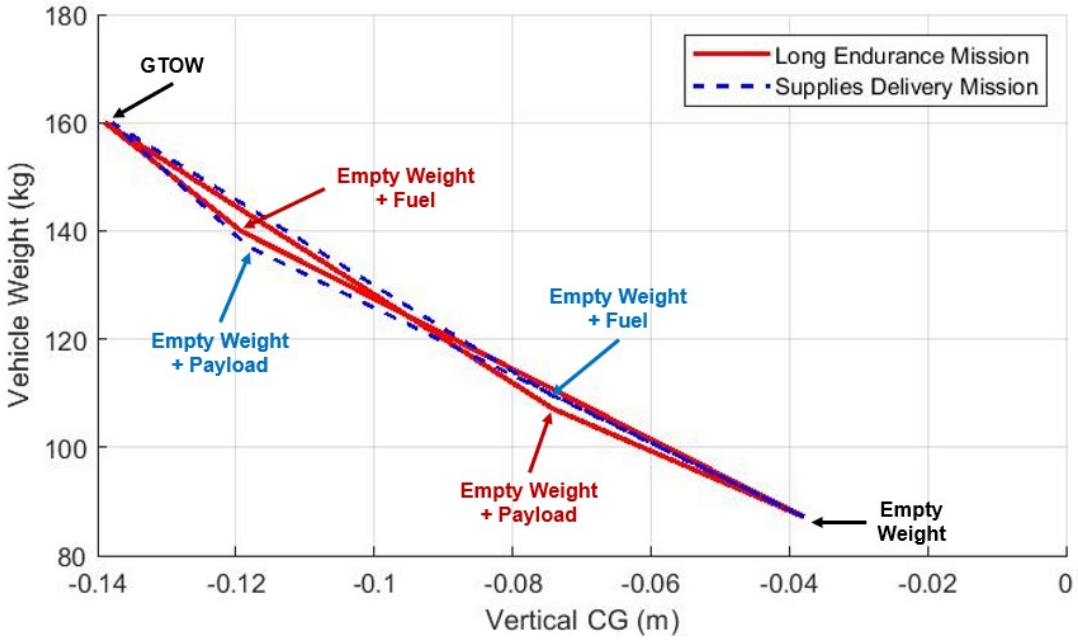

Fig 81: Vehicle Vertical CG Variation (Positive Upward)

14 Summary

The 2024 Student Design Competition Request for Proposals issued by the Vertical Flight Society and DEVCOM ARL desired the development of a new multi-mission, modular UAS. This report has outlined the proposed design of *Ibis* - a low weight, low cost, and multi-mission single main rotor UAS that exceeds both RFP mission requirements with one vehicle configuration. *Ibis'* rotor system and aerodynamics enables exceptional performance - high efficiency blades, streamlined fuselage, and a low vibration and stable articulated rotor system. These aerodynamics allow *Ibis* to loiter for nearly 11 hours while following the long-endurance mission profile. Converting mission configurations easily in under 10 minutes, *Ibis* also exceeds the supplies-delivery mission requirements, capable of delivering 59 kg (130 lb) of payload. The vehicle is designed with proven high TRL technologies throughout - including a flight proven recuperating turbine engine and fixed skid landing gear. These systems are all assembled together into a user-friendly design so that disaster survivors can safely get the rescue supplies and connectivity they deserve. *Ibis* solves the need for small, versatile, and high-performing unmanned vertical lift aircraft that can be rapidly deployed to any situation. With the onset of any disaster, *Ibis* will be the first vehicle out and the last one back.

References

[1] Smith, A. B., "2022 U.S. billion-dollar weather and climate disasters in historical context," Jan. 10 2022.

[2] ZenaDrone Inc., *The Various Uses of Emergency Drones for Disaster Management*, 2022.

[3] Johnson, W., "NDARC NASA Design and Analysis of Rotorcraft," Tech. rep., NASA Ames Research Center, Moffett Field, CA, 2023.

[4] Nagaraj, V. and Chopra, I., *Preliminary Design of Rotorcraft*, University of Maryland College Park, 2023.

[5] Johnson, W., *Rotorcraft Aeromechanics*, Cambridge University Press, 2013.

[6] "AR56 — Structural Design Requirements (Helicopters)," Tech. rep., Naval Air Systems Command Department of Navy, 1970.

[7] Wiesner and Kohler, "Tail Rotor Design Guide," *USAAMRDL Technical Report 73-99*, 1974.

[8] Li, Q., Yang, Y., Yu, X., and Li, H., "A 700 Whkg1 Rechargeable Pouch Type Lithium Battery," *Chinese Physics Letters*, March 2023.

[9] Huggins, R., *Advanced Batteries: Materials Science Aspects*, chap. 1.4.3 The Maximum Theoretical Specific Energy (MTSE), Springer, 2009.

[10] "RC-Turboshaft Specifications," *Jakadofsky Jet Engines*, 2022.

[11] "PBS TS100 Specification Sheet," *PBS Aerospace*, 2020.

[12] "TA200TP 'Talon' Turboprop Engine," *TurbAero*, 2023.

[13] "Stuttgart Engineering Engine Specifications," *Stuttgart Engineering*, 2015.

[14] "Technical Specifications," *Papiz Turbine*, 2023.

[15] Bamsey, I., "UAV Turbines UTP50R 50 hp recuperated gas turbine," *UAV Turbines*, Jan 2017.

[16] Prando, D., Brenna, A., Diamanti, M., et al., "Corrosion of Titanium: Part 1: Aggressive Environments and Main Forms of Degradation," *Journal of Applied Biomaterials Functional Materials*, Vol. 15, No. 4, 2017, pp. e291–e302.

[17] Chernoff, M., "Analysis and design of Skid Gears for level landing," *Journal of the American Helicopter Society*, Vol. 7, No. 1, 1962, pp. 33–39.

[18] Tadakuma, K., Tani, Y., and Aso, S., "Effect of Fuselage Cross Section on Aerodynamic Characteristics of Reusable Launch Vehicles," *Open Journal of Fluid Dynamics*, Vol. 06, No. 03, 2016, pp. 222–233.

[19] Figat, M., Kwiek, A., and Seneńko, K., "Aerodynamic Design of the Strake for the Rocket Plane in Tailless Configuration," *29th Congress of the International Council of the Aeronautical Sciences, ICAS 2014*, 2014.

[20] "Vector-600," *UAV Navigation*, 2024, https://www.uavnavigation.com/products/autopilots/vector-600.

[21] "FLIR Duo® Pro R," *Teledyne FLIR*, 2023, https://www.flir.com/support/products/duo-pro-r/Documents.

[22] "Innoviz360," *Innoviz Technologies*, Jun 19 2023, https://innoviz.tech/innoviz360.

[23] "ROG Strix SCAR 16 (2023) G634," *ASUS*, Jun 19 2023, https://shop.asus.com/us/90nr0d91-m001b0-g634jy.html.

[24] "14 CFR Part 91 Subpart C § 91.209," Feb. 1996.

[25] Prouty, R. W., *Helicopter Performance, Stability, and Control*, Krieger Publishing Company, Malabar, FL, 2002.

[26] Sridharan, A., Govindarajan, B., and Chopra, I., "A Scalability Study of the Multirotor Biplane Tailsitter Using Conceptual Sizing," *Journal of the American Helicopter Society*, Vol. 65, Jan 2019.

[27] "Air BP Products Handbook," *BP*, 2011, Original work published [2008] Accessed on [5-28-2024], Recovered using Internet Archive.

[28] Gill, H. and Lee, S., "Development of New Empirical Rotor Broadband Noise Prediction Models for Urban Air Mobility Applications," *AIAA SciTech Forum*, Orlando, FL, Jan 8-10 2024.

[29] Harris, F. and Scully, M., "Rotorcraft Cost Too Much." *Journal of the American Helicopter Society*, Vol. 43, No. 1, 1998.

[30] "2002 Request for Proposals : "Light Helicopter Upgrade Program" 19th Annual Student Design Competition for Undergraduate and Graduate Students Sponsored by American helicopter Society and Bell Helicopter Textron," *The Vertical Flight Society*, 2002.

[31] "Yamaha Unmanned Helicopter R-Max," *Yamaha Motor Co. LTD*, December 2023.

[32] "Schiebel next-generation UAV Camcopter," *New Atlas*, May 2015.